Noname manuscript No.
(will be inserted by the editor)

Unveiling the faint ultraviolet Universe

A. Zanella[1,2] · C. Zanoni[2] · F. Arrigoni-Battaia[3] · A. Rubin[2] · A. F. Pala[2] · C. Peroux[2,4] · R. Augustin[5] · C. Circosta[2,6] · E. Emsellem[2,7] · E. George[2] · D. Milaković[2] · R. van der Burg[2] · T. Kupfer[8]

arXiv:1910.01194v2 [astro-ph.IM] 25 Jan 2021

Received: date / Accepted: date

Abstract With this paper we participate to the call for ideas issued by the European Space Agency to define the Science Program and plan for space missions from 2035 to 2050. In particular we present five science cases where major advancements can be achieved thanks to space-based spectroscopic observations at ultraviolet (UV) wavelengths. We discuss the possibility to (1) unveil the large-scale structures and cosmic web in emission at redshift $\lesssim 1.7$; (2) study the exchange of baryons between galaxies and their surroundings to understand the contribution of the circumgalactic gas to the evolution and angular-momentum build-up of galaxies; (3) constrain the efficiency of ram-pressure stripping in removing gas from galaxies and its role in quenching star formation; (4) characterize the progenitor population of core-collapse supernovae to reveal the explosion mechanisms of stars; (5) target accreting white dwarfs in globular clusters to determine their evolution and fate. These science themes can be addressed thanks to UV (wavelength range $\lambda \sim 90-350$ nm) observations carried out with a panoramic integral field spectrograph (field of view $\sim 1 \times 1$ arcmin^2), and medium spectral (R = 4000) and spatial ($\sim$ 1" – 3") resolution. Such a UV-optimized instrument will be unique in the coming years, when most of the new large facilities such as the Extremely Large Telescope and the James Webb Space Telescope are optimized for infrared wavelengths.

Keywords ESA Voyage 2050 · Space missions: ultraviolet instrument · Integral field spectrograph · Galaxies · White dwarfs · Supernovae

1 Introduction

The European Space Agency (ESA) has started planning the next cycle of space missions by establishing the long-term ESA Science Program Voyage 2050. This follows the current plan (Cosmic Vision, extending up to 2035) and is the framework in which ESA space missions from 2035 up to 2050 will be defined. In order to keep the Science Program a bottom-up process and gather inputs from the scientific community about the science themes that should be covered by the Voyage 2050 planning cycle, ESA has issued

[1]Istituto Nazionale di Astrofisica, Vicolo dell'Osservatorio 5, 35122 Padova (Italy) - Tel.: +39 0498 293507 - E-mail: anita.zanella@inaf.it · [2]European Southern Observatory, Karl-Schwarzschild-Str. 2, 85748 Garching bei München (Germany) · [3] Max-Planck-Institut für Astrophysik, Karl-Schwarzschild-Str 1, 85748, Garching bei München, Germany · [4] Aix Marseille Université, CNRS, LAM (Laboratoire d'Astrophysique de Marseille) UMR 7326, 13388, Marseille, France · [5] Space Telescope Science Institute, 3700 San Martin Drive, Baltimore, MD, 21218, USA · [6] Department of Physics & Astronomy, University College London, Gower Street, London WC1E 6BT, United Kingdom · [7] Univ. Lyon, Univ. Lyon1, ENS de Lyon, CNRS, Centre de Recherche Astrophysique de Lyon UMR5574, F-69230 Saint-Genis-Laval (France) · [8] Kavli Institute for Theoretical Physics, University of California, Santa Barbara, CA 93106, USA

a call for White Papers in March 2019. In this paper we discuss five science cases, spanning different fields of astrophysics, presenting scientific challenges that can be addressed with a space-based mission in 2035 – 2050, conducting spectroscopic observations in the ultraviolet (UV), a wavelength regime that is not accessible from the ground.

- By detecting the intergalactic medium in emission it will be possible to directly unveil the cosmic web, whose existence is predicted by current theories of structure formation. This will enable studies of the exchange of baryons between galaxies (and quasars) and their surroundings, unveiling how the halo gas contributes to the evolution of galaxies and what mechanisms drive the galaxy angular momentum build-up through cosmic time. Finally, multiple detections of the intergalactic medium in emission will provide measurements of the UV background, a critical quantity used in simulations of galaxy formation, yet still poorly constrained in observations (Section 2.1, 2.2).
- Observations of the neutral gas distribution (by mapping the Lyman-α emission) in low-redshift galaxy cluster members will clarify the efficiency with which ram-pressure stripping removes the gas from galaxies and the role of the environment in quenching star formation. These observations will be crucial to understand how and when the red sequence of galaxies is assembled in dense environments. These observations will be key in interpreting high redshift observations, where currently the Lyman-α is more easily accessible (Section 2.3).
- By observing statistical samples of supernovae in the UV it will be possible to characterize the progenitor population of core-collapse supernovae, providing the initial conditions for explosion models and allowing the community to progress in the understanding of the explosion mechanism of stars, as well as the final stages of stellar evolution (Section 2.4).
- By targeting populations of accreting white dwarfs in globular clusters it will be possible to constrain the evolution and fate of these stars and investigate the properties of the most compact systems with the shortest orbital periods which are expected to be the brightest low-frequency gravitational wave sources. The possibility will also be explored that accreting white dwarfs are progenitors of Type Ia supernovae, which are fundamental sources to constrain cosmological distances and the current models for dark energy (Section 2.5).

A UV-optimized telescope (wavelength range $\lambda \sim 90$ - 350 nm), equipped with a panoramic integral field spectrograph with a large field of view (FoV $\sim 1 \times 1$ arcmin^2), with medium spectral (R = 4000) and spatial ($\sim$ 1" – 3") resolution will allow the community to simultaneously obtain spectral and photometric information of the targets, and tackle the science questions presented in this paper (Section 5). The information-rich nature of the datasets provided by such an integral field spectrograph will represent a resource with considerable legacy value for the scientific community. Additionally, these observations will open up completely new areas of the parameter space, allowing the proposed mission to have a great potential for serendipitous discoveries.

In the coming years, when most of the new large facilities such as the Extremely Large Telescope (ELT) and the James Webb Space Telescope (*JWST*) will focus on the infrared (IR) wavelength range, and the Hubble Space Telescope (*HST*) will not be operational anymore, a mission in the UV with the capability of observing spectroscopically large areas of the sky will be unique. In synergy with the Atacama Large Millimeter Array (ALMA), the ELT instruments, and Square Kilometer Array (SKA), but also with other space-based missions such as the Advanced Telescope for High Energy Astrophysics (*Athena*) and the Laser Interferometer Space Antenna (*LISA*) it will allow us to push further our current understanding of the Universe.

We present the main science themes to be addressed in the coming decades in Section 2; we compare the characteristics of the proposed straw-man mission and instrument with other UV space missions in Section 3 and its synergies with future facilities in Section 4; finally in Section 5 we sketch the high-level technical characteristics of the proposed instrument and address potential technological challenges.

2 Science cases

2.1 Unveiling large-scale structures in emission at $z \lesssim 1.7$

The current paradigm of large-scale structure formation predicts the presence of an intricate net of gaseous filaments connecting galaxies (e.g., White et al. 1987, Bond et al. 1996). The existence of this cosmic web, also known as intergalactic medium (IGM; Meiksin 2009), is until now confirmed only indirectly by observations of the large-scale structures traced with galaxy surveys at low redshift and by studies of the Lyman-α (Lyα) forest in absorption against background quasars. Direct imaging of the cosmic web, probing its properties and evolution through cosmic history, will represent a major breakthrough for cosmology. Directly detecting the IGM in this way, is predicted to be very challenging (surface brightness in Lyα predicted to be $\mathrm{SB_{Ly\alpha}} \sim 10^{-19} - 10^{-20}\,\mathrm{erg\,s^{-1}\,cm^{-2}\,arcsec^{-2}}$; Gould and Weinberg 1996; Bertone and Schaye 2012; Witstok et al. 2019) because of the expected low densities for such gas ($n_\mathrm{H} \lesssim 0.01\,\mathrm{cm^{-2}}$) and the budget of ionizing photons in the ultraviolet background (UVB; e.g., Haardt and Madau 2012). A direct detection of the IGM appears to be so far elusive even with top-notch current facilities on 10m class telescopes (e.g., Gallego et al. 2018; Wisotzki et al. 2018), such as the Multi Unit Spectroscopic Explorer (MUSE; Bacon et al. 2010) and the Keck Cosmic Web Imager (KCWI; Morrissey et al. 2012). Ground-based instruments can target the Lyα emission only above the atmospheric cut-off ($z \gtrsim 1.7$) and thus fight against a strong cosmological surface brightness dimming that scales as $(1+z)^{-4}$.

Astronomers have tried to bypass these limitations by searching the IGM signal around quasars. A quasar is expected to act as a flashlight, photoionizing the surrounding medium out to large distances. The ionized gas would then recombine, emitting as the main product hydrogen Lyα photons in copious amounts (e.g. Rees 1988; Haiman and Rees 2001). The Lyα glow around quasars should then be boosted up to $\mathrm{SB_{Ly\alpha}} > 10^{-19}\,\mathrm{erg\,s^{-1}\,cm^{-2}\,arcsec^{-2}}$, and therefore be within the reach of state-of-the-art instruments (Cantalupo et al. 2005; Kollmeier et al. 2010).

Following this idea, several works targeted extended Lyα emission around high-redshift quasars to constrain the physical properties of the diffuse gas phases out to intergalactic scales around individual objects (Tumlinson et al. 2017, Hu and Cowie 1987; Heckman et al. 1991; Møller et al. 2000; Weidinger et al. 2004, 2005; Christensen et al. 2006; Cantalupo et al. 2014; Martin et al. 2014; Arrigoni Battaia et al. 2016; Farina et al. 2017, 2019). For example, at $z \sim 3$, it is now possible with MUSE to easily ($\sim$ 1 hour on source; surface brightness limit of $\mathrm{SB_{Ly\alpha}^{1\ arcsec^2}} \sim 10^{-18}\,\mathrm{erg\,s^{-1}\,cm^{-2}\,arcsec^{-2}}$) uncover the emission within 50 projected kpc from the targeted quasar, and to detect it up to distances of $\sim$ 80 projected kpc (Borisova et al. 2016; Arrigoni Battaia et al. 2019a). Notwithstanding these achievements when targeting individual quasars, it is evident that detections of diffuse emission at intergalactic distances (> 100 kpc) at high z are favored when additional active companions are present in close proximity (Hennawi et al. 2015; Arrigoni Battaia et al. 2019a, 2018), or much more sensitive observations are conducted (> 10 hours). Recent studies in the literature started to show new approaches in unveiling the IGM emission, passing from the observations of individual quasars to (i) short (Cai et al. 2018; Arrigoni Battaia et al. 2019b) or extremely long integrations ($\gg$ 40 hours; Lusso et al. 2019) of multiple high-redshift quasars, or overdensities hosting quasars (Cai et al. 2017), and (ii) stacking of ultra deep observations of several galaxies (Gallego et al. 2018; Wisotzki et al. 2018; Leclercq et al. 2020). At face value, the detection of large-scale gas in emission still relies on the presence of active galaxies.

In spite of the aforementioned difficulties in observing the IGM, state of the art integral field unit (IFU) spectrographs, by pushing the sensitivity of observations to $\mathrm{SB_{Ly\alpha}} \sim 10^{-19} - 10^{-20}\,\mathrm{erg\,s^{-1}\,cm^{-2}\,arcsec^{-2}}$, started to open new opportunities for the study of the gas distributed over large scales at high redshift. To study the large scale structures at the more accessible low-z Universe, a new-generation space mission optimized for UV observations is needed to complement the ongoing efforts at high redshift. By routinely detecting the IGM in emission at $z \lesssim 1.7$, this instrument will allow us to achieve the following science goals:

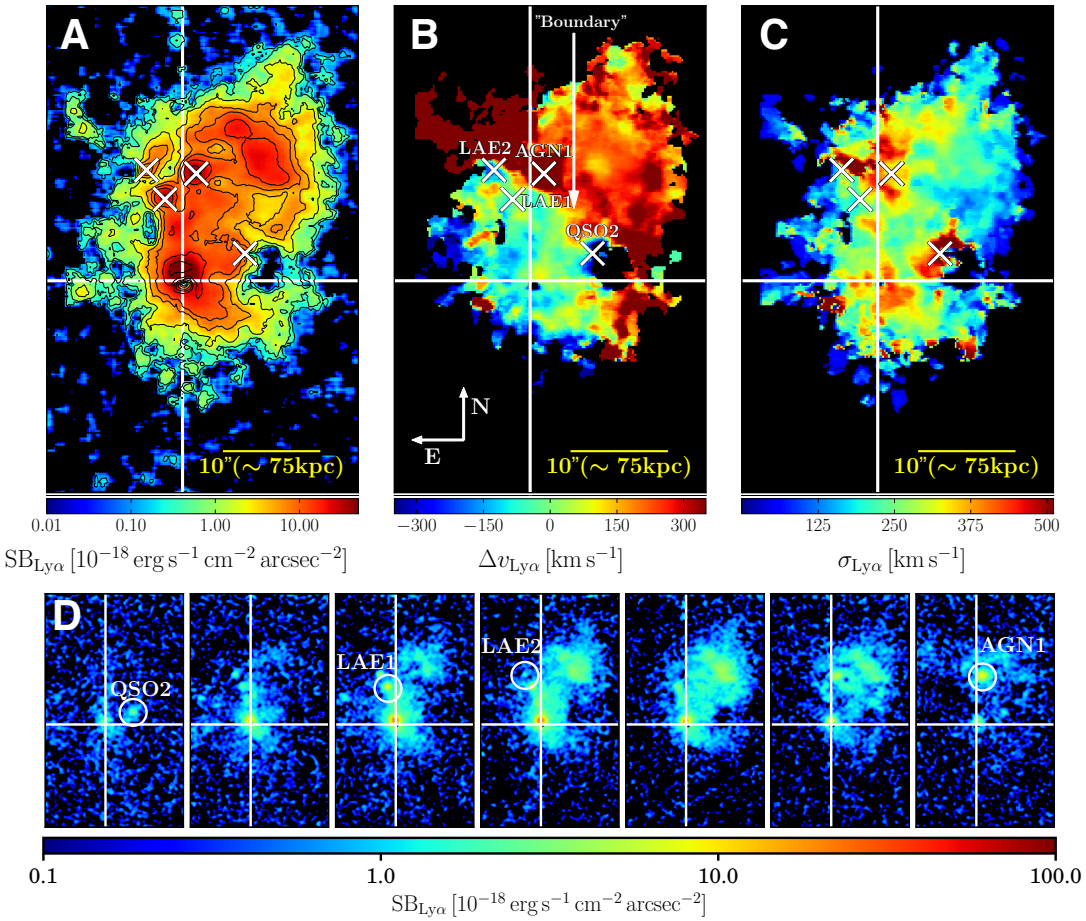


Fig. 1: An example of current large-scale structures detected in Lyα around quasars with VLT/MUSE at high redshift: the enormous Lyα nebula (ELAN) around the $z = 3.164$ quasar SDSSJ 1020+1040 (figure adapted from Arrigoni Battaia et al. 2018). **(A)** "optimally-extracted" Lyα surface brightness map obtained after subtraction of the quasar point-spread-function and continuum. The black contours indicate the isophotes corresponding to a signal-to-noise ratio of S/N = 2, 4, 10, 20, 30, 50, and 100. This image reveals an extremely bright nebula (SB$_{Ly\alpha} \sim 10^{-17}$ erg s^{-1} cm^{-2} arcsec^{-2}) extending on the NW side of the quasar. Additional four strong Lyα emitters (diagonal crosses) are associated with the quasar, and the nebular emission. Two of these sources have been spectroscopically confirmed as AGN, making this system the third known quasar triplet at high z. **(B)** flux-weighted velocity-shift map with respect to the systemic redshift of the quasar obtained from the first-moment of the flux distribution. A velocity shear between the SE and NW portion of the nebula is evident. The transition region is referred to as the "Boundary". **(C)** velocity dispersion map obtained from the second-moment of the flux distribution. Regions of higher dispersion ($\sigma_{Ly\alpha} \approx 430$ km s^{-1}) are visible in proximity of the three AGN, but overall the Lyα nebula shows quiescent kinematics ($\sigma_v < 270$ km s^{-1}). **(D)** Each cut-out image (same size as A, B, and C) shows the surface brightness map of the ELAN within a 3.75 Å layer (3× MUSE sampling) in the wavelength range 5058 Å $\lesssim \lambda \lesssim$ 5084 Å (from left to right). In all of the panels (A, B, C, D) the large white cross indicates the position of the quasar prior to PSF subtraction. Currently, similar large-scale emission cannot be probed at low z ($z \lesssim 1.7$) because of the absence of appropriate facilities.

– Connect the dots at low redshift: test our current view of the matter distribution at low z by detecting the cosmic web in emission (through rest-frame UV emission lines) surrounding galaxies and quasars. This is crucial in our understanding of structure formation as we can currently only rely on galaxies as tracers of the distribution of large-scale structures at low z (Malavasi et al., 2017).

- Directly study the properties (e.g., density, metallicity) of the IGM in emission, complementing the information acquired from studies of the Lyα forest.
- Provide measurements of the UV background at low z thanks to multiple detection of the IGM in emission, building up independent constraints from the statistics of the IGM in absorption. The UV background is a critical quantity used in all simulations and models of structure formation, but it is still poorly constrained observationally. Its precise determination is key for our understanding of galaxy formation and evolution (e.g., Khaire and Srianand 2019, Faucher-Giguère 2020).
- Study of the gas kinematics within the large-scale structures surrounding galaxies, allowing a direct characterization of the galaxy angular momentum build-up through cosmic time.

2.1.1 The need for space-based UV observations

Recent works show that the most efficient and effective way to detect emission extending to hundreds of kpc scales around high-z quasars and galaxies is the use of wide-field IFU instruments (e.g., Figure 1; Arrigoni Battaia et al. 2018). Space-based, wide-field spectroscopic observations in the wavelength range $\lambda \sim 90 - 350$ nm will allow us to achieve our scientific goals. Specifically, a space-based instrument is needed to observe the Lyα transition at low z ($z \lesssim 1.7$), where the cosmological surface brightness dimming is less severe. Assuming similar properties for the gas, it will be possible to target sources with 16× lower surface brightness at $z \sim 0.5$ with respect to $z \sim 3$. Furthermore, a wide field of view (1×1 arcmin^2, which corresponds to hundreds of kpc at $z \lesssim 1.7$) is needed to efficiently image the large-scale structures that subtend large areas on the sky. As we are interested in detecting large scale structures with very low surface brightness, large pixels (e.g. $\sim$ 1 arcsec) are preferred to enhance sensitivity (as in e.g. KCWI; Morrissey et al. 2012).

2.2 Probing the emission of the Circumgalactic Medium around galaxies

Understanding the complex mechanisms regulating galaxy formation is one of the main questions today in cosmology and astrophysics. The question of how galaxies gather gas to sustain star formation is of particular interest, as it sheds light on the fact that the star formation rate (SFR) has been declining from $z \sim 2$ while diffusely distributed hydrogen is still the dominant component for the total baryonic mass budget (as compared to hydrogen in stars, Madau and Dickinson 2014). The outflowing and accreting gas interacts around galaxies on scales up to hundreds of kpc (the Circumgalactic Medium, CGM). Studying the CGM is fundamental to understand the cosmic baryon cycle (Steidel et al. 2010, Shull et al. 2014, Tumlinson et al. 2017, Péroux and Howk 2020) and it will provide key constraints on the question of galaxy formation and evolution. Absorption spectroscopy has already provided insights on the distribution and the chemical composition of the CGM gas from a statistical point of view, given that typically only one line of sight per galaxy can be studied due to the scarcity of background quasars in the vicinity of galaxies (Noterdaeme et al. 2012, Pieri et al. 2014, Quiret et al. 2016, Rahmani et al. 2016, Krogager et al. 2017, Augustin et al. 2018, Hamanowicz et al. 2020). Therefore, mapping the CGM in emission is the important next step to reach a full understanding of these complex regions.

2.2.1 The need for space-based UV observations

To achieve the science goals presented above it is key to detect and map different lines (e.g. Lyα, CIV, OVI, CVI, OVIII) arising from the CGM of low-redshift galaxies. The signal (surface brightness) scales with $(1+z)^{-4}$ so that lower redshift observations are considerably easier in turn requiring space-born UV facilities to measure rest-frame UV lines. IFU-like capabilities are key for obtaining maps and kinematic reconstructions of the gas in the halos of galaxies. A field of view of $\sim 1 \times 1$ arcmin^2 will cover most

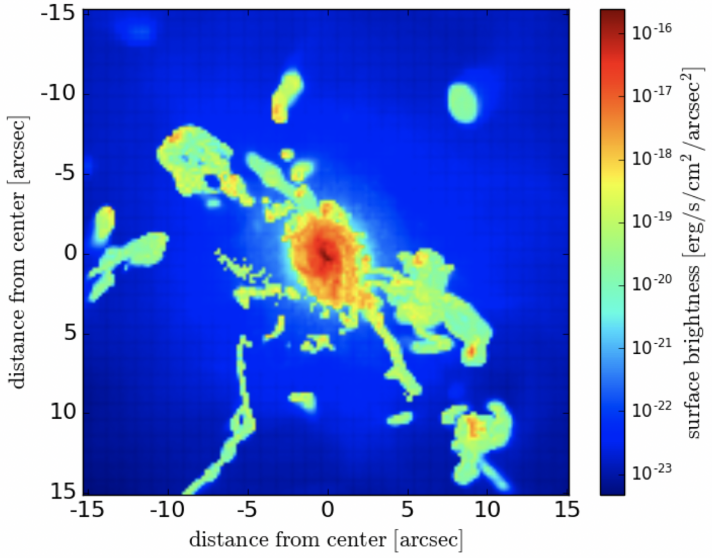


Fig. 2: Example of a mock Lyα CGM halo around a $z = 0.7$ galaxy, from RAMSES hydrodynamical cosmological simulations (Augustin et al., 2019). The Lyα line is at 206 nm and 1" $\sim$ 7 kpc at the redshift of this source. The CGM surface brightness levels shown in this map will be within reach of the proposed UV instrument.

of the CGM region of a galaxy at $z \sim 1$. Modest spatial resolution (to increase sensitivity) and spectral resolution (R $\sim$ 4000) are sufficient. Such a program will be complementary to similar high-redshift projects that make use of extremely large ground-based telescopes (i.e. ELT/HARMONI). An example of mock Lyα CGM halo at $z = 0.7$ from dedicated RAMSES cosmological hydrodynamical simulations is shown in Figure 2 (Augustin et al., 2019).

2.3 Ram-pressure stripping and quenching in galaxy clusters

The existence of a well defined separation between massive, red, early-type, quiescent galaxies and blue, late-type, actively star-forming objects is a key leverage for the current modeling of galaxy formation and evolution. Nowadays, "normal" galaxies are thought to assemble their mass through a secular process of star formation in a relatively steady state, forming a "Main Sequence" up to high redshift (e.g. Daddi et al. 2007, Speagle et al. 2014) and following a tight gas-star formation rate (SFR) density relation ("KS" relation, Schmidt 1959, Kennicutt 1998). Deviations from this dynamic equilibrium may occur in short starbursting events (typically associated with major mergers, Sanders and Mirabel 1996) or due to the cessation of star formation ("quenching"). Both these deviations from equilibrium are poorly understood: why do galaxies suddenly ignite the formation of thousands of stars per year? Why do they stop forming stars? The deviations from the Main Sequence and the KS relation might be connected: the merger of gas-rich objects may first result in a burst of star formation, followed by a drop of the SFR and the subsequent quenching of the galaxy. The results of this process might be the compact, quiescent galaxies observed at $z \lesssim 2$ (e.g. Cimatti et al. 2008, Toft et al. 2014). However, it is still debated what is the mechanism responsible for stopping star formation and how galaxies are maintained quiescent for several Gyrs.

An additional piece of the puzzle is the correlation between galaxy color (and morphology) with both local environment and stellar mass (Dressler 1980, Bell et al. 2004, Peng et al. 2010). The environmental

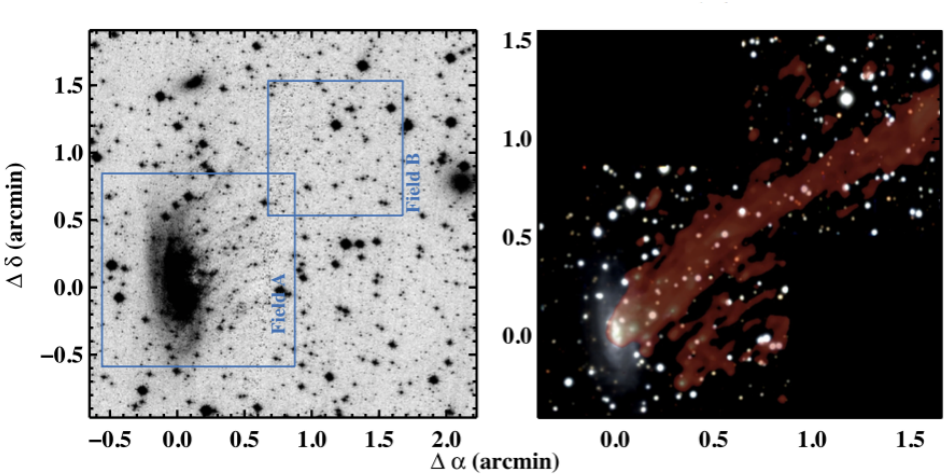


Fig. 3: Example of a local cluster member undergoing ram pressure stripping observed with VLT/MUSE: ESO137-001 at $z = 0.016$ (Fumagalli et al., 2014). **Left**: HST/ACS image in the F475W filter with, superposed, the MUSE field of view at the two locations targeted by the observations. **Right**: RGB color image obtained combining images extracted from the MUSE data cube in three wavelength intervals ($\lambda = 500 - 600$ nm for the B channel, $\lambda = 600 - 700$ nm for the G channel, and $\lambda = 700 - 800$ nm for the R channel). A map of the Hα flux is overlaid in red using a logarithmic scale, revealing the extended gas tail that originates from the high-velocity encounter of ESO137-001 with the intra-cluster medium.

dependence seems to indicate that not only internal, but also external, physical processes play a role in shaping the star formation of galaxies at all cosmic ages (Boselli et al. 2006, Blanton and Moustakas 2009). Internal mechanisms such as feedback from supernovae and active galactic nuclei (AGN, e.g. Hopkins et al. (2012), Croton et al. 2006), dynamical stabilization (Martig et al. 2009), and gravitational heating (Johansson et al., 2009) are deemed responsible for suppressing and quenching star formation at all densities. Environmental processes in the form of ram pressure or viscous stripping, tidal interactions (Gunn and Gott, 1972), and the consumption of the galaxy's gas reservoir by star formation without further replenishment from the cosmic web because of accumulation of hot plasma inducing shocks and heating up infalling gas (e.g. Larson et al. 1980, Peng et al. 2015; Dekel and Birnboim 2006) seem to be key players in shaping the observed color bimodality within galaxy clusters and groups, especially at the faint end of the galaxy luminosity function.

In the local Universe, the smoking gun of the role of ram pressure stripping in quenching star formation is the disturbed gas content of galaxy cluster members. Radio surveys at 21 cm revealed the HI deficiency of spiral galaxies in overdense environments, especially in the vicinity of the cluster core (Haynes 1985) and more recently the molecular gas deficiency has also been reported (Fumagalli et al. 2009, Boselli and Gavazzi 2014). Furthermore, these galaxies often show disturbed gas morphologies and tails visible both in Hα (Figure 3) and UV continuum (e.g. Gavazzi and Jaffe 1985, Fumagalli et al. 2014, Fossati et al. 2016).

However, at high redshift ($1 \lesssim z \lesssim 1.5$) there is still no consensus on the influence of the environment on galaxies' gas content (Aravena et al. 2012, Dannerbauer et al. 2017, Coogan et al. 2018). This is mainly driven by detections that are either lacking, or limited to the most gas-rich members. Galaxies undergoing ram pressure stripping are ideal laboratories to constrain the efficiency with which gas can be removed and star formation is quenched. Observations of galaxy clusters and groups at different redshifts are therefore key to understand how and when the red sequence of galaxies is assembled in dense environments.

2.3.1 The need for space-based UV observations

To study quenching mechanisms in dense environments and the origin of galaxy red sequence, a space-based instrument with a large field of view ($\sim 1 \times 1$ arcmin^2), exquisite sensitivity, and a spectral coverage $\lambda \sim 90 - 350$ nm is needed. This part of the spectrum includes the Lyα emission line at redshift $z \lesssim 1.7$. Lyα traces the neutral gas, which is expected to be the bulk of the material stripped by ram pressure, and is expected to be $> 10\times$ brighter than Hα (e.g. Scarlata et al. 2009). Mapping the Lyα emission with a wide-field spectrograph would allow us to trace stripped gas out to large distances from the galaxy (~ 500 kpc at $z = 1$) and to unveil gas tidal tails $\gtrsim 10\times$ fainter than the Hα ones, therefore targeting also the less massive cluster members. The detection of other emission lines (e.g. CIII, OI, HeII, MgII) would allow us to constrain the density, temperature, and metallicity of the ionized gas. The comparison of the Lyα and Hα fluxes would also give information about the powering mechanisms of Lyα (e.g. shocks, star-formation, cooling), still an unknown issue. Are cluster members mainly fast rotators, as expected if their star formation has been quenched by the interaction with the intra-cluster medium? Or are more violent interactions (Toloba et al., 2011) responsible for the stripping of their gas? A resolution of $R \sim 4000$, would enable us to probe the kinematics of stars and gas simultaneously, and such questions would be thoroughly addressed.

The stripped gas is expected to be mainly in the cold atomic phase, but it could be heated and change phase once it interacts with the hot gas confined within the potential well of the cluster. Complementary multi-frequency observations will allow us to reach a comprehensive picture of these phenomena: the molecular phase is detectable through CO (ALMA), SKA will target the cold HI gas at 21 cm, the hot gas phase is visible in the X-rays (*Athena*), while the ionized gas phase will be probed by ELT instruments.

2.4 Supernovae

Core collapse supernovae are the most common form of death for massive stars (Li et al., 2011). These events are the end-stage of massive stellar evolution, and are responsible for the chemical enrichment of the galaxy. While many supernovae have been discovered and observed, the characteristics of the stars that explode are still a mystery. Observationally it has been established that massive stars ($> 8M_\odot$) end their lives as a core-collapse supernova. However, theoretical models have not succeeded in reproducing the observed explosion properties, and more importantly cannot self-consistently explode the star without an artificially induced ignition (Burrows, 2013). The progenitors of core-collapse supernovae have been positively identified for a handful of events (Smartt et al., 2009; Smartt, 2015). The progenitor's characteristics are one of the major open questions which must be addressed in order to progress our understanding of the explosion mechanism of stars, as well as the final stages of stellar evolution.

The most robust technique for identifying progenitors is with high-resolution images taken before the explosion. This technique has been successfully employed a handful of times using primarily *HST* images taken before the events (Smartt et al., 2004; Maund et al., 2011; Van Dyk, 2017). Some core-collapse supernovae seem to originate from red supergaint stars, but there is also an example of a Type IIb originating from a yellow hypergiant (Maund et al., 2011; Bersten et al., 2012). Two limitations prevent this technique from significantly advancing the field in the future: first, an image of the region prior to the explosion is needed; second, it is necessary to wait for $5-10$ years until the supernova fades to below the progenitors' luminosity in order to confirm that the star terminally exploded and disappeared. Even when the second criterion is satisfied, some doubt remains as the star could be enshrouded in a high-extinction dust. Given these limitations, pre-explosion imaging is unlikely to increase the number of identified progenitors by orders of magnitude in the future.

The solution is to use semi-analytic models which have been developed in recent years (Waxman et al., 2007; Nakar and Sari, 2010; Rabinak and Waxman, 2011; Sapir and Waxman, 2017). These models

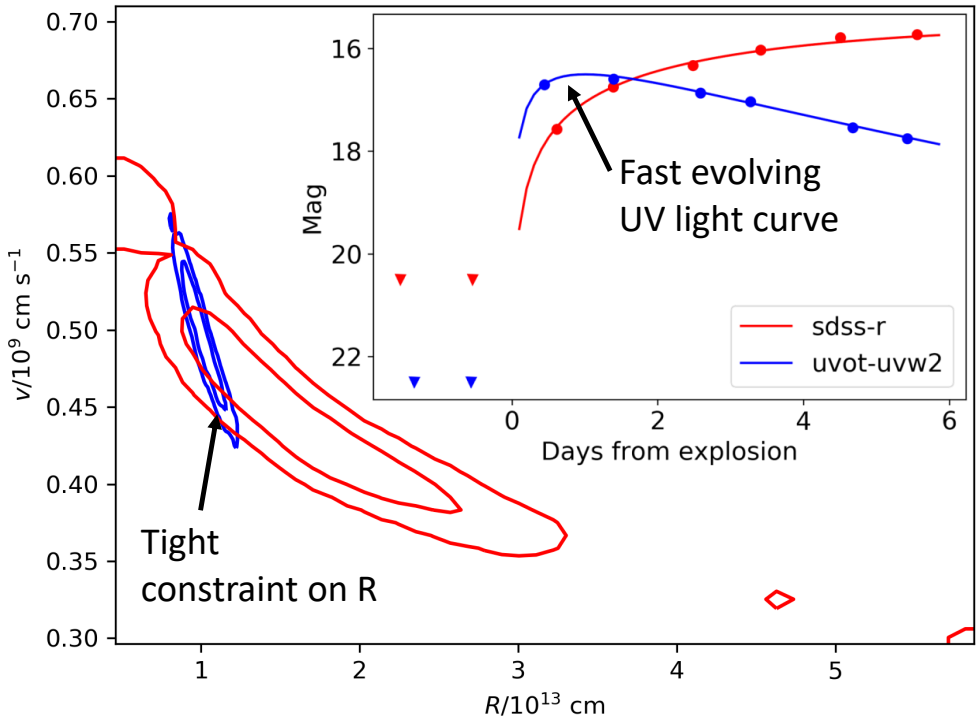


Fig. 4: Constraints on radius and ejecta velocity (energy per unit mass of the explosion). In the inset we show a simulated light-curve as it would appear in UVOT-UVW2 and SDSS-r. The simulation is of an $R = 10^{13}$ cm progenitor observed with $\sim$ 1 day cadence. Note the faster rise of the UV light-curve. The contours represent 68% and 95% of the probability of the fit to the UV and visual bands separately. The UV is clearly more sensitive to the progenitor's radius than visual bands.

can relate the observed light curve of a core-collapse supernova to the progenitor's radius and the velocity of the ejecta (energy per unit mass of the explosion). These models can be applied to light curves of events which do not have pre-explosion images, and therefore have the potential to increase by orders of magnitude the number of identified progenitors. The hot ejecta ($> 10^4$ K) cools rapidly during the first days after the explosion. Because in the UV and optical wavelengths the blackbody spectrum is in the Rayleigh-Jeans regime, the UV light-curve evolves more rapidly than longer optical wavelengths (e.g. R-band). Shock-cooling models can only be applied to data taken during the first few days after explosions, therefore the rapid evolution of the UV light curve is critical for constraining the progenitor's properties. Rubin and Gal-Yam (2017) showed that visual-band wavelengths cannot constrain the progenitor's radius meaningfully, but that UV coverage at moderate (0.5−1 day cadence) can constrain the progenitor's radius to 20%. With a significant number of supernovae observed in the UV, it will be possible to measure the progenitor population of core-collapse supernovae. These will provide the initial conditions for explosion models, and will provide benchmarks against which to design and test these simulations.

UV spectroscopy will also play a major role in understanding the surface composition of the progenitors. It has been shown that many supernovae have a circumstellar material surrounding the star from before the explosion (Gal-Yam et al., 2014; Yaron et al., 2017; Khazov et al., 2016). At the moment of first light, this material becomes highly ionized by the tremendous luminosity and temperature of the first photons of the explosions. After a timescale of hours to days the bulk of the supernovae ejecta sweeps up this material. During this window strong, highly ionized emission lines have been observed (e.g. OIII, HeII). These can be related back to the surface composition of the progenitor star in the last period before

it exploded. Groh (2014) showed that the most informative lines are in the UV, e.g. CIV λ1548 – 1551, HeII λ1640, and NVI λ1718.

2.4.1 The need for space-based UV observations

To achieve our science goals we will need photometry of magnitude 20 sources with a cadence of 0.5 – 1 day. By simultaneously obtaining the spectra of our targets (with magnitude down to 20) with a signal-to-noise of 10 we will measure the temporal evolution of the UV flux, and the strength and equivalent widths of the transient emission lines CIV λ1548 – 1551, HeII λ1640, and NVI λ1718, to achieve the science goals mentioned above (Figure 4).

2.5 Accreting white dwarfs in globular clusters: testing the models of compact binary evolution

Accreting white dwarfs (WDs), namely binaries in which a WD accretes from a main sequence star or a degenerate companion, are a strategical tool to probe the physical properties of the Universe and to test fundamental physical theories. The thermonuclear ignition of WDs following the interaction with a binary companion results in Type Ia supernovae (SNe Ia), which are fundamental yardsticks to constrain cosmological distance scales (Branch and Tammann, 1992) and the existence of dark energy (Riess et al., 1998; Perlmutter et al., 1999). Moreover, the most compact systems with orbital periods below one hour are among the brightest known low frequency gravitational wave sources and will be used to verify the performance of the space-based gravitational wave mission *LISA* and to calibrate the detector for future gravitational wave source discoveries (Kupfer et al., 2018). It is therefore critical to understand the evolution and final fate of accreting WDs.

Currently, there are several significant discrepancies between the predictions of population synthesis models and the observed properties of accreting WDs. In particular (i) the interplay between the angular momentum loss mechanisms driving the evolution of accreting WDs at different orbital period regimes is poorly understood (e.g. Schreiber et al., 2016; Belloni et al., 2020); (ii) the evolutionary path followed by the most compact systems is unknown (e.g. Green et al., 2018); (iii) the final fate of accreting WDs and the pathway leading to SN Ia explosions is still not clear (see e.g. Maoz and Mannucci, 2012, for a review). Solving these discrepancies is essential before the theoretical models can be sensibly applied to more complex binaries, such as black hole and neutron star binaries, X-ray transients, and SN Ia progenitors.

Accreting WDs are predicted to be numerous in globular clusters ($\simeq 100 - 200$ per cluster, Ivanova et al. 2006; Knigge 2012). Globular clusters (GCs) are therefore a unique laboratory where to carry out statistical binary population synthesis studies for populations of accreting WDs with known distance, metallicity, and age (Knigge, 2012; Belloni et al., 2016). By observing populations of accreting WDs in GCs we will explore the following science cases:

- Constrain the rates of orbital angular momentum losses. To test the prediction of the current models, measurements of the angular momentum loss rates at different orbital periods ($P_{\rm orb}$) are needed. However, the long timescale over which the orbital period changes typically prevents direct measurements from being obtained. A proxy for the mean mass accretion rate and, in turn, for the angular momentum loss rate is the WD effective temperature ($T_{\rm eff}$, Townsley and Bildsten 2003; Bildsten et al. 2006), as it is determined by the compressional heating of the accreted material (Sion, 1995; Townsley and Bildsten, 2004). While several thousand accreting WDs are known, accurate temperatures are only measured for $\simeq 80$ systems, obtained from ultraviolet *HST* observations (Bildsten et al., 2006; Townsley and Gänsicke, 2009; Pala et al., 2017). In this sample, only systems with a period $70\,{\rm min} < P_{\rm orb} < 150\,{\rm min}$ show an angular momentum loss in agreement with model predictions, while all the others show discrepancies of more than one order of magnitude with the theory (Fig. 5).

- The formation of the most compact systems. Two main populations of accreting WDs are known: (1) the systems with main-sequence and brown-dwarf donors (cataclysmic variables, CVs) with orbital periods in the range $60\,\mathrm{min} \lesssim P_{\mathrm{orb}} \lesssim 2\,\mathrm{d}$ and (2) the systems with helium stars or helium-core WDs as donors (AM CVn stars) with orbital periods $P_{\mathrm{orb}} \lesssim 60\,\mathrm{min}$. The formation of AM CVn stars is still poorly understood and evolutionary models currently predict different formation scenarios (Nelemans et al., 2010). Particularly, it has been suggested that AM CVn could descend from CVs in which the donor is nuclear evolved, i.e. enriched of CNO processed material. To observationally constrain different models it is key to study the chemical composition (e.g. N/O and N/C ratios) of the donor (Nelemans et al., 2010). Establishing the fraction of CVs with evolved donor could provide an upper limit on the number of AM CVn that are expected to form through this channel (see e.g. Pala et al., 2020), thus yielding a valuable observational test for the formation of these compact systems.
- Accreting WDs and SN Ia progenitors. Both CVs and AM CVns are intimately connected to the formation of SNe Ia. In fact, CVs with nuclear evolved donors undergo a phase of stable hydrogen shell burning during which the WD mass grow (possibly to the Chandrasekhar limit) and AM CVns accrete He-rich material from their degenerate donors, potentially triggering a SN Ia via the double-detonation mechanism (Bildsten et al., 2007; Fink et al., 2010). Determining the masses of these systems through a fit of the UV spectrum provides firm statistical constraints for the above scenarios and could finally confirm the potential of these systems as SN Ia progenitors. Also the rotation rates of accreting WDs are a critical parameter in the pathway leading to SNe Ia explosion. Absorption features from the photosphere of the WD accretor, which are only cleanly detected in the UV, can be used to measure the rotational velocity and determine whether the WD is spun up by accretion, allowing the WD to exceed the Chandrasekhar limit without triggering the SN explosion.

2.5.1 The need for space-based UV observations

The population of accreting WDs in GCs provides a statistically significant sample of systems spanning the whole orbital period distribution and will allow us to carry out stringent tests for the current models of compact binary evolution (e.g. Knigge et al., 2002). Accreting WDs have typical temperatures $T_{\mathrm{eff}} \gtrsim 10\,000\,\mathrm{K}$ and their spectral energy distribution peaks in the ultraviolet. In other wavelength domains, the emission is dominated by the disc (in the optical) or a boundary layer at the WD surface (in the X-rays). Space-based ultraviolet spectroscopy is therefore the only method to access and fully characterize the physical properties of these stars (e.g Szkody et al., 2002; Gänsicke et al., 2006; Sion et al., 2008; Pala et al., 2017). Moreover, the majority of the main sequence and red giants stars are cool (Teff < 7000 K) and their emission peaks in the optical and/or in the near-infrared. For this reason, in the UV wave range GCs appear vastly less crowded than in the optical (see e.g. fig. 1 from Knigge et al. 2002). The proposed UV IFU would provide the possibility to (i) deblend the denser environments and study those sources that would be inaccessible to optical studies owing to crowding and (ii) obtain, in one shot, a spectrum of the detectable UV sources in the field of view.

From the knowledge of the GC distance, the WD T_{eff} can be measured via a spectral fit to the ultraviolet data with synthetic atmosphere models thus providing a direct measurement of the angular momentum loss rate in the system (Townsley and Gänsicke, 2009). The spectral fit to ultraviolet data also provides the WD photospheric abundances which reflect the composition of the donor star, via the detection of strong emission and absorption resonance lines of C, N, O and Si (e.g. Nv 1240 Å, Civ 1549 Å, and Oi 1150, 1302 Å; Gänsicke et al. 2003; Morales-Rueda et al. 2003; Sion et al. 2006) which are not accessible in the optical. A single ultraviolet spectrum thus provides information on both the WD accretor and the donor star, offering a unique insight into the composition of the donor and the prior evolution of the system. A spectral fit to ultraviolet data also yields accurate mass determinations, thus providing firm statistical constraints for the double-detonation scenario and the mass growth in CVs, finally confirming the potential of these systems as SN Ia progenitors. Finally, rotation rates of accreting WDs have so far

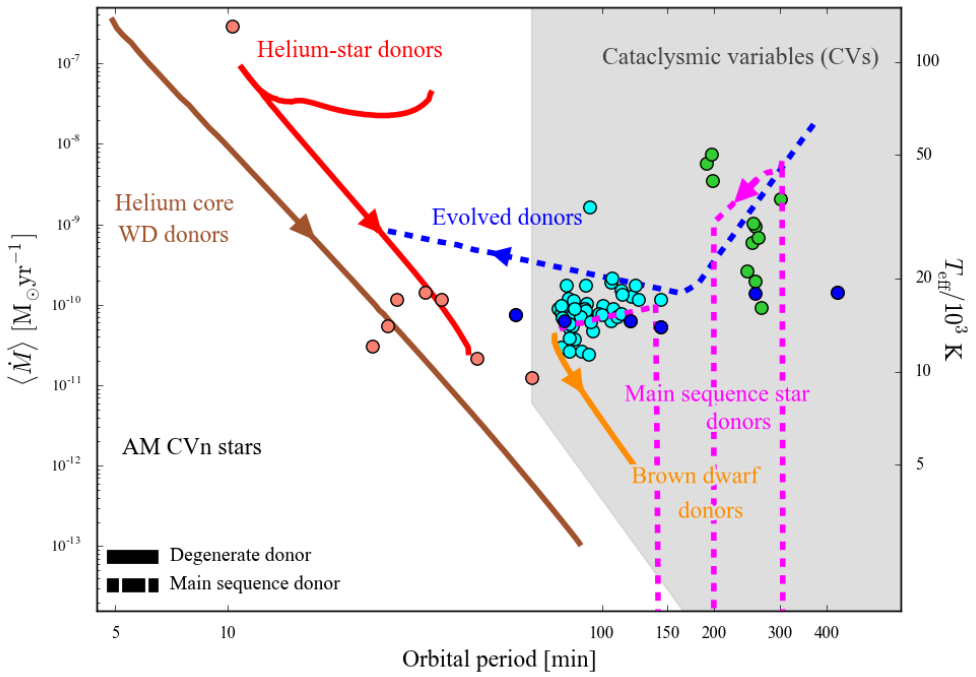


Fig. 5: Effective temperatures of short-period (cyan) and long-period (green) CV WDs, AM CVns (pink) and systems with evolved donors (blue) (Bildsten et al., 2006; Townsley and Gänsicke, 2009; Pala et al., 2017). The WD $T_{\rm eff}$ (right y-axis) directly translates into a measurement of the average mass accretion rate ($\langle \dot{M} \rangle$, left y-axis), which is a measurement of the angular momentum loss rate in the system. While the observations of short-period CVs (cyan) agree reasonably well with the theoretical evolutionary tracks (Bildsten et al., 2006; Yungelson, 2008; Nelemans et al., 2010; Pala et al., 2017), long-period CVs (green), AM CVns (pink) and systems with evolved donors (blue) are poorly studied and the few systems observed uncover major discrepancies between observations and models.

been measured only in a handful of systems (e.g. Sion et al., 1994; Long et al., 2004). A resolving power of $\simeq$ 4000 is sufficient to measure rotation rates $v \sin i \gtrsim 100$ km/s, thus providing robust observational constraints on the response of WDs to the accretion of mass and angular momentum.

3 Comparison with other space instruments

A wide-field, IFU-like instrument on board a space telescope optimized for UV observations (λ = 90−350 nm) will allow the community to simultaneously obtain photometric and spectroscopic observations with exquisite sensitivity in a wavelength regime that is not accessible from the ground, making it a unique instrument to tackle the scientific questions presented in Section 2 as well as many other topics. There are currently only two spectrographs on board *HST* that cover a wavelength range similar to the one that we propose (COS and STIS), one such spectrograph was launched on the stratospheric balloon FIREBall, and two new ones are currently being proposed to be on board of CETUS and the *LUVOIR* telescope (LUMOS). In the following, we discuss why these spectrographs are not suitable to achieve the science cases described in Section 2.

***HST*/COS**: the wavelength coverage of this spectrograph (λ = 90 - 320 nm) is similar to the one that we propose and it was designed to obtain spectroscopy of faint point-like sources (e.g. stars, quasars) with a resolving power R ∼ 1500 – 24000 (Green et al., 2012). The extremely small field of view of COS

(2.5″ diameter) however prevents observations of large patches of the sky and the possibility of observing extended objects, a critical requirement for all science cases presented in this document. Some of our science questions overlap with those that motivated COS, but the way we want to address them is substantially different. As an example, the question of whether the cosmic web exists and how baryons from galaxies interact with the surrounding medium can be tackled by COS by studying absorption spectra of intergalactic gas (e.g. Lyα forest, highly ionized absorption lines such as OIV, NV), whereas we propose to address this issue by studing the intergalactic medium in emission, through the detection of Lyα halos extended across hundreds of kpc (and possibly other rest-frame UV emission lines). Similarly, COS is suitable to study white dwarfs, cataclysmic variables, and binary stars in the Milky Way. However the instrument that we propose will open up the new possibility to target these sources in globular clusters, dramatically increasing the statistics and efficiency of the observations.

***HST*/STIS**: this spectrograph and imaging camera covers the far- and near-UV wavelength range (λ = 115 – 310 nm, Woodgate et al. 1998). Spatially-resolved observations can be performed through slitless spectroscopy, but the resolving power (R $\leq$ 2500) is too low to achieve our science goals (R $\gtrsim$ 4000 is needed). Furthermore, the low throughput of STIS ($\lesssim$ 10%) only allows observation of the brightest targets (the limiting magnitude V = 20.6 for an A0V star can be observed with a signal-to-noise ratio of 10 in 1 hour on source) and is not enough to reach the faint surface brightness levels required to achieve our goals (e.g. $SB_{Ly\alpha} \sim 10^{-19} - 10^{-20}$ erg s^{-1} cm^{-2} arcsec^{-2}, see Section 2.1).

FIREBall-2: this is a multi-object spectrograph operating in the UV and flying on a stratospheric balloon at an altitude of 40 km (Lemaitre et al., 2019). It follows the experiments started with FIREBall-1 aimed at detecting the faint and diffuse emission of the intergalactic medium. It is equipped with a fiber IFU (300, 8" fibers). Part of the scientific motivation for FIREBall overlaps with the one proposed here (Section 2.1), but FIREBall only observes a limited wavelength range (200 - 210 nm) and targets the Lyα emission line at $z \sim 0.6 - 0.7$. We propose to cover a larger wavelength range ($\sim$ 90 – 350 nm), pushing the observations of Lyα up to z $\sim$ 1.7, starting to bridge the local and high-redshift Universe. Furthermore the field of view of FIREBall-2 is not contiguous (i.e. the fibers need to be placed in separate positions) and the spatial ($\sim$ 4") and spectral (R $\sim$ 2000) resolution are not enough to achieve our science goals. The overall throughput of the instrument on FIREBall is $\sim$ 5% that is not enough to reach the low surface brightness level needed by our science goals. Finally, since this instrument works on a stratospheric balloon, its operations strongly depend on weather conditions and aeronautical rules, and observations can only be performed for a few consecutive nights each time. The possibilities to get the long exposures needed to probe faint emissions are therefore limited. These kind of operational conditions cannot sustain a large demand from the astronomical community, but are key for testing new UV technologies and space-validate sub-components in a zero-gravity environment. The FIREBall team has also proposed to NASA to fund a new mission, ISTOS (Martin et al., 2011), designed at studying the faint UV emission from the circum- and inter-galactic medium leveraging in particular on the development of new detectors with improved capabilities (i.e. higher quantum efficiency and lower noise thanks to the use of EMCCDs).

***LUVOIR*/LUMOS** and **CETUS**: these are both UV multi-object spectrographs that have been proposed for future missions. LUMOS will cover the far-UV to visible wavelength range (λ = 100 – 1000 nm), is currently under study, and is a candidate instrument for the future *LUVOIR* space mission (France et al., 2017). CETUS instead is a Probe Mission Concept that NASA has selected for consideration (Kendrick et al., 2019). It will enable parallel observations by the UV multi-object spectrograph ($\lambda \sim 180 - 350$ nm) and near-UV/far-UV camera ($\lambda 115 - 400$ nm) which will operate simultaneously but with separate field of views. Thanks to their large field of view ($2' \times 2'$ LUMOS, and $17' \times 17'$ CETUS) both these instruments will be able to observe hundreds of targets at once. However the field of view covered by LUMOS and CETUS, as opposed to the IFU instrument that we are proposing, will not be contiguous. A 100% coverage of a large field of view to a high depth is critical to efficiently achieve our science goals, such as contiguously map the extended emission of the cosmic web and galaxy halos, the extended tidal tails around galaxy cluster members, globular clusters that host populations of accreting

white dwarfs. A discontiguous field of view drastically reduces the efficiency of the observations and the discovery potential. Additionally, compared to a multi-object spectrograph that can only perform pointed observations, the IFU instrument that we propose will provide thousands of spectra with a single pointing and will therefore have a unique potential for serendipitous discoveries. Finally, LUMOS is designed to observe at the diffraction limit and CETUS will have a spatial resolution $\lesssim 0.3''$, conditions that would prevent us from achieving the extremely low surface brightness levels needed by our science cases.

Additionally the **MESSIER surveyor**, a small UV ($\lambda = 150 - 1000$ nm) space mission designed to explore the Universe down to very low surface brightness fluxes ($\sim 34 - 37$ mag arcsec^{-2}), is under development and has recently received initial funding from the French Space Agency CNES (Valls-Gabaud and MESSIER Collaboration, 2017). Although some of the science drivers of this surveyor overlap with those proposed in Section 2 (e.g. the detection of the cosmic web in emission), MESSIER will be an imager equipped with a set of filters, whereas we are proposing an IFU instrument that will allow the community to simultaneously obtain photometric and spectroscopic information of the targets. With such an IFU the community could follow-up spectroscopically the most promising targets imaged by facilities like MESSIER. Having access to spectroscopy down to such low surface brightness will enlarge the parameter space that can be explored and greatly increase the discovery potential.

4 Synergies

In the next two decades all the major facilities are expected to operate at red, IR, and radio wavelengths (e.g. *JWST*, ELT, SKA). A window on the UV will therefore offer a complementary view at shorter wavelengths and will have strong synergies with these facilities. It will be critical to conduct follow-up observations in the UV regime, at a time when *HST* will not be operational anymore. An IFU-like instrument operating in the UV will also provide targets that can then be followed-up with the ELT (e.g. the gas stripped from galaxy cluster members observed in Lyα can be observed in [OII] and Hα with ELT/HARMONI providing information on the ionized gas). Furthermore most of the science questions presented here have synergies with future major facilities such as SKA at longer wavelengths (e.g. to detect the HI gas stripped in cluster members and the cosmic web around galaxies) and will benefit from targets identified by *Euclid* and the Rubin Observatory in large field imaging. There are also synergies with ALMA, should it still be operational (e.g. the gas stripped by cluster members might be detected both in the neutral phase through Lyα emission with our proposed instrument and in the molecular phase with ALMA). Finally synergies with *Athena* and *LISA* will enhance the discovery potential (e.g. *Athena* will unveil the hot gas phase stripped by cluster members and present in the circumgalactic medium visible in the X-rays, while *LISA* will detect the gravitational waves produced by the most compact accreting white dwarfs with short orbital periods).

5 Technical concept

In this Section, we present some key design areas for a system compliant with the proposed science theme. We notice that a dedicated space mission is not strictly required and an instrument hosted on another future spacecraft may suffice. Finally, we highlight that a system study has not been performed, as this goes beyond the scope of the proposal. Critical technologies are highlighted via a brainstorming process and discussions with relevant experts. Given the main characteristics of the telescope (Table 1), the dedicated space mission fits an ESA M-size type.

Table 1: Main (range of) parameters of the telescope and instrument.

Aperture	0.9 - 1.1 m
F-number	F/5 - F/15
Field of view	1×1 arcmin^2
Wavelength range	90 – 350 nm (preferred) 100 – 300 nm (minimum requirement)
Spectral resolution	average R = 4000
Spectral sampling	0.5 Å per spectral bin
Spatial sampling	0.5" × 1" per spaxel
Spatial resolution (FWHM)	2" – 3"
Throughtput	$\gtrsim$ 25% over the whole wavelength range

5.1 Type of Telescope and Instrument

Current space-based facilities are optimized to detect point-like sources such as stars or distant galaxies, rather than extended low surface brightness targets (Trujillo and Fliri, 2016). To reach the surface brightness of $\sim 10^{-19}$ erg s^{-1} cm^{-2} arcsec^{-2} required by our science cases, a telescope with a diameter of $\sim$ 0.9 – 1.1 m and a relatively fast optics (F-number $\sim$ F/5 – F/15) is needed (Valls-Gabaud and MESSIER Collaboration, 2017). Ideally, the F-number should have even faster values. That would require technologies with currently a very low technology readiness level (TRL), such as curved detectors.

A UV integral field unit (IFU) is the only available option to achieve the science goals of the previous Sections. Part of the technology that has already been developed for the ground-based Multi Unit Spectroscopic Explorer (MUSE) on the Very Large Telescope (VLT) and that is currently being upgraded for BlueMUSE (λ = 350 – 600 nm, Richard et al. 2019) can be adapted for this project. Insights on the performance of IFUs in space can also be obtained from *JWST*/NIRSpec (Deshpande et al., 2018), when launched, although NIRSpec will operate at IR wavelengths.

The proposed IFU extends the capabilities of such type of instruments toward bluer wavelengths, λ = 90 – 350 nm, not observable from the ground, targeting different science cases. It has a single instrumental setup (i.e. fixed spectral and spatial setup), which simplifies the overall fore-optics. A rapid response mode is necessary to carry out observations of transients (Section 2.4). We summarize in Table 1 the main characteristics of the instrument, with their reasonable range.

5.2 Mass

Due to the complexity and extent of the optics, IFUs tend to be heavy instruments, an important constraint for a space mission. The mass will be one of the main design drivers. Section 5.6 proposes a possible way to greatly simplify the optics. That is a solution with low TRL and requiring further development.

5.3 Thermal Control

Another design driver is given by the thermal environment, as it is often the case for optics in space. On one hand, for the detectors, cryogenic temperatures are required to maximize the performance. On the other hand, it is preferable to perform UV observations with a temperature of the optics above 260 K to prevent absorption on the reflective surfaces, given that UV systems are sensitive even to mono-layers

of contaminants (LUVOIR team, 2018). An operating temperature in the range 270 K – 290 K is recommended because it reduces the risks linked to launch shocks and facilitates mission development as testing, alignment, and mirrors polishing and figuring can be performed on the ground without cooling facilities, with a smaller number of iterations and eventually lower complexity.

Wavefront stability requires the temperature of the optics to be controlled within 10^{-2} K. A sun-synchronous orbit would be preferable to avoid eclipses and operate in a more stable environment. However, this is not a strict constraint and UV observations have extensively been performed by other telescopes (e.g. *HST*) on different orbits.

5.4 Vibrations Control

The wavefront stability also calls for isolation and damping of vibrations sources. Dedicated precision mechanisms on the optics or micronewton thrusters, following the heritage of Gara and LISA Pathfinder (Armano et al., 2016), are potential disturbance avoidance solutions (Dennehy and Alvarez-Salazar, 2018). In fact, they remove the need of reaction wheels, which are strong sources of disturbance also during operation.

5.5 Materials

In line with decades of warm optics design, the traditional choices for the material of the mirrors are Zerodur™ and ULE™ thanks to their high stability. Silicon Carbide (SiC) is also an option. In fact, while it poses some challenges on the surface finishing and requires more stringent constraints on the thermal control, it has significant advantages in terms of controllability thanks to its superior strength. A set of actuators (e.g. piezo-stacks) annealed in the SiC substrate, allows wavefront errors to be compensated in several load conditions, including on-ground testing in 1-g.

Space-based instruments that are currently operational at UV wavelengths have a throughtput $< 25\%$ in the wavelength range $\lambda = 200 - 400$ nm (e.g. WFC3 UVIS filters on board *HST*). To achieve our goals a throughtput $\gtrsim 25\%$ is needed. Such performance is currently hindered by the decrement of reflectivity below 110 nm of the typical mirror coatings (e.g. silver and gold), (LUVOIR team, 2018). Aluminium has in principle a good reflectivity down to wavelengths of ~ 100 nm, but it has the known tendency to oxidation. There are however promising studies on this subject (Balasubramanian et al. 2017, Quijada et al. 2017) that point to the use of protective layers to prevent aluminum oxidation from degrading the performance.

5.6 Detectors

To achieve the proposed science goals we need to reach very low surface brightness objects. As an example, to detect the Lyα emission from the circumgalactic medium we need to observe $\mathrm{SB_{Ly\alpha}} \sim 10^{-19}\,\mathrm{erg\,s^{-1}\,cm^{-2}\,arcsec^{-2}}$. Given the characteristics of the proposed telescope and instrument (Table 1), this translates to a detection threshold of $\sim 0.2 - 1$ $\mathrm{e^-\ pixel^{-1}\ hr^{-1}}$. Currently the main limitation to reach such low detection thresholds is given by the readout noise of the detectors ($\sim 2 - 3$ $\mathrm{e^-}$ for both CMOS and CCDs). However, there are ongoing studies focusing on enhancing UV detector performances and reducing the readout noise. On the CCD side, EMCCDs that use avalanche gain on the readout are currently available. This technology has been tested in sub-orbital flights on FIREBall (Hamden et al. 2016, 2019).

In the CMOS detector market, 8k × 8k CMOS devices exist already, although they are not optimized yet for the UV and they still have a relatively high readout noise. A study to develop a CMOS detector

with readout noise below 0.15 e^- is currently in progress with results from the simulation of the silicon circuit showing single-photon sensitivity (Stefanov et al. 2020). Another promising technological development is in black silicon nano-structures with self induced junctions, allowing effective QE above 100% without external amplification in the UV wavelength range (Garin et al. 2019). A combination of these technologies would lead to a powerful new detector optimized for low-noise UV observations.

An alternative to building an optical IFU with traditional detectors is the use of an imaging camera together with a "spectrometer on a chip" detector based on MKID technology. These detectors measure the energy of every photon that hits the detector, and are already in use for the DARKNESS spectrometer (Meeker et al., 2018). MKIDs have no dark current or readout noise in the traditional sense, as they measure thousands to millions of quasiparticles for every photon that hits. However, they are subject to quasiparticle fluctuations, limiting the precision with which the energy of the photons can be measured and in turn the achievable spectral resolution. In fact, the spectral resolution that they can currently achieve is only $R < 100$, but theoretically it could be much higher and there are already proposals for using this technology in space (Rauscher et al., 2016). This technology however trades decreased optics complexity for increased cryogenic complexity, as MKIDs require a superconducting layer and therefore extreme cryogenic temperatures ($\approx$1 K).

6 Conclusions

An entire new window on the Universe is opened by exploring its UV-range with high spatial and spectral resolution. We have showcased several different science questions to be addressed in the time frame of Voyage 2050, and highlighted how our approach will ensure ample opportunities for serendipitous discoveries.

The ideal instrument to answer the proposed scientific questions is a UV-optimized, wide-field IFU. It could be hosted by a future telescope or alternatively by a new M-size mission and it will be the only UV IFU in space. Designing and building such a complex system will encourage the technological development of several areas, including material science, data acquisition and reduction, UV detector technology, and micro-vibrations mitigation.

Finally, by focusing on the UV wavelength range after and during an epoch when the largest available facilities have been operating at red and IR wavelengths (e.g. *JWST*, ELT), this instrument will open up a new discovery space and will be suitable to work in synergy with the main available observatories now in development such as *Athena*, the ELT, and SKA.

Acknowledgements We are grateful to J. Kosmalski, J. Spyromilio, Chian-Chou Chen, and F. Lelli for useful discussions and inputs.

Conflict of interest

The authors declare that they have no conflict of interest.

References

Aravena M, Carilli CL, Salvato M, Tanaka M, Lentati L, Schinnerer E, Walter F, Riechers D, Smolcić V, Capak P, Aussel H, Bertoldi F, Chapman SC, Farrah D, Finoguenov A, Le Floc'h E, Lutz D, Magdis G, Oliver S, Riguccini L, Berta S, Magnelli B, Pozzi F (2012) MNRAS 426(1):258–275, DOI 10.1111/j.1365-2966.2012.21697.x, 1207.2795

Armano M, Audley H, Auger G, Baird JT, Bassan M, Binetruy P, Born M, Bortoluzzi D, Brandt N, Caleno M, Carbone L, Cavalleri A, Cesarini A, Ciani G, Congedo G, Cruise AM, Danzmann K, de Deus Silva M, De Rosa R, Diaz-Aguiló M, Di Fiore L, Diepholz I, Dixon G, Dolesi R, Dunbar N, Ferraioli L, Ferroni V, Fichter W, Fitzsimons ED, Flatscher R, Freschi M, García Marín AF, García Marirrodriga C, Gerndt R, Gesa L, Gibert F, Giardini D, Giusteri R, Guzmán F, Grado A, Grimani C, Grynagier A, Grzymisch J, Harrison I, Heinzel G, Hewitson M, Hollington D, Hoyland D, Hueller M, Inchauspé H, Jennrich O, Jetzer P, Johann U, Johlander B, Karnesis N, Kaune B, Korsakova N, Killow CJ, Lobo JA, Lloro I, Liu L, López-Zaragoza JP, Maarschalkerweerd R, Mance D, Martín V, Martin-Polo L, Martino J, Martin-Porqueras F, Madden S, Mateos I, McNamara PW, Mendes J, Mendes L, Monsky A, Nicolodi D, Nofrarias M, Paczkowski S, Perreur-Lloyd M, Petiteau A, Pivato P, Plagnol E, Prat P, Ragnit U, Raïs B, Ramos-Castro J, Reiche J, Robertson DI, Rozemeijer H, Rivas F, Russano G, Sanjuán J, Sarra P, Schleicher A, Shaul D, Slutsky J, Sopuerta CF, Stanga R, Steier F, Sumner T, Texier D, Thorpe JI, Trenkel C, Tröbs M, Tu HB, Vetrugno D, Vitale S, Wand V, Wanner G, Ward H, Warren C, Wass PJ, Wealthy D, Weber WJ, Wissel L, Wittchen A, Zambotti A, Zanoni C, Ziegler T, Zweifel P (2016) Sub-Femto-g Free Fall for Space-Based Gravitational Wave Observatories: LISA Pathfinder Results. Phys Rev Lett 116:231101, DOI 10.1103/PhysRevLett.116.231101, URL https://link.aps.org/doi/10.1103/PhysRevLett.116.231101

Arrigoni Battaia F, Hennawi JF, Cantalupo S, Prochaska JX (2016) The Stacked LYα Emission Profile from the Circum-Galactic Medium of z $\sim$ 2 Quasars. ApJ 829:3, DOI 10.3847/0004-637X/829/1/3, 1604.02942

Arrigoni Battaia F, Prochaska JX, Hennawi JF, Obreja A, Buck T, Cantalupo S, Dutton AA, Macciò AV (2018) Inspiraling halo accretion mapped in Lyα emission around a z $\sim$ 3 quasar. MNRAS 473:3907–3940, DOI 10.1093/mnras/stx2465, 1709.08228

Arrigoni Battaia F, Hennawi JF, Prochaska JX, Oñorbe J, Farina EP, Cantalupo S, Lusso E (2019a) QSO MUSEUM I: a sample of 61 extended Ly α-emission nebulae surrounding z $\sim$ 3 quasars. MNRAS 482:3162–3205, DOI 10.1093/mnras/sty2827, 1808.10857

Arrigoni Battaia F, Obreja A, Prochaska JX, Hennawi JF, Rahmani H, Bañados E, Farina EP, Cai Z, Man A (2019b) Discovery of intergalactic bridges connecting two faint z $\sim$ 3 quasars. A&A 631:A18, DOI 10.1051/0004-6361/201936211, 1909.00829

Augustin R, Péroux C, Møller P, Kulkarni V, Rahmani H, Milliard B, Pieri M, York DG, Vladilo G, Aller M, Zwaan M (2018) Characterizing the circum-galactic medium of damped Lyman-α absorbing galaxies. MNRAS 478(3):3120–3132, DOI 10.1093/mnras/sty1287, 1805.05960

Augustin R, Quiret S, Milliard B, Péroux C, Vibert D, Blaizot J, Rasera Y, Teyssier R, Frank S, Deharveng JM, Picouet V, Martin DC, Hamden ET, Thatte N, Pereira Santaella M, Routledge L, Zieleniewski S (2019) Emission from the circumgalactic medium: from cosmological zoom-in simulations to multi-wavelength observables. MNRAS 489(2):2417–2438, DOI 10.1093/mnras/stz2238, 1909.02575

Bacon R, Accardo M, Adjali L, Anwand H, Bauer S, Biswas I, Blaizot J, Boudon D, Brau-Nogue S, Brinchmann J, Caillier P, Capoani L, Carollo CM, Contini T, Couderc P, Daguisé E, Deiries S, Delabre B, Dreizler S, Dubois J, Dupieux M, Dupuy C, Emsellem E, Fechner T, Fleischmann A, François M, Gallou G, Gharsa T, Glindemann A, Gojak D, Guiderdoni B, Hansali G, Hahn T, Jarno A, Kelz A, Koehler C, Kosmalski J, Laurent F, Le Floch M, Lilly SJ, Lizon JL, Loupias M, Manescau A, Monstein C, Nicklas H, Olaya JC, Pares L, Pasquini L, Pécontal-Rousset A, Pelló R, Petit C, Popow E, Reiss R, Remillieux A, Renault E, Roth M, Rupprecht G, Serre D, Schaye J, Soucail G, Steinmetz M, Streicher O, Stuik R, Valentin H, Vernet J, Weilbacher P, Wisotzki L, Yerle N (2010) The MUSE second-generation VLT instrument 7735:773508, DOI 10.1117/12.856027

Balasubramanian K, Hennessy J, Raouf N, Nikzad S, Del Hoyo J, Quijada M (2017) Mirror coatings for large aperture UV optical infrared telescope optics 10398:103980X, DOI 10.1117/12.2274794

Bell EF, McIntosh DH, Barden M, Wolf C, Caldwell JAR, Rix HW, Beckwith SVW, Borch A, Häussler B, Jahnke K, Jogee S, Meisenheimer K, Peng C, Sanchez SF, Somerville RS, Wisotzki L (2004)

GEMS Imaging of Red-Sequence Galaxies at z ∼ 0.7: Dusty or Old? ApJL 600:L11–L14, DOI 10.1086/381388, astro-ph/0308272

Belloni D, Giersz M, Askar A, Leigh N, Hypki A (2016) MOCCA-SURVEY database I. Accreting white dwarf binary systems in globular clusters - I. Cataclysmic variables - present-day population. MNRAS 462(3):2950–2969, DOI 10.1093/mnras/stw1841, 1607.07619

Belloni D, Schreiber MR, Pala AF, Gänsicke BT, Zorotovic M, Rodrigues CV (2020) Evidence for reduced magnetic braking in polars from binary population models. MNRAS 491(4):5717–5731, DOI 10.1093/mnras/stz3413, 1910.06333

Bersten MC, Benvenuto OG, Nomoto K, Ergon M, Folatelli G, Sollerman J, Benetti S, Botticella MT, Fraser M, Kotak R, Maeda K, Ochner P, Tomasella L (2012) The Type IIb Supernova 2011dh from a Supergiant Progenitor. ApJ 757(1):31, DOI 10.1088/0004-637X/757/1/31, URL http://iopscience.iop.org/0004-637X/757/1/31

Bertone S, Schaye J (2012) Rest-frame ultraviolet line emission from the intergalactic medium at $2 \leq z \leq 5$. MNRAS 419:780–798, DOI 10.1111/j.1365-2966.2011.19742.x, 1008.1791

Bildsten L, Townsley DM, Deloye CJ, Nelemans G (2006) The Thermal State of the Accreting White Dwarf in AM Canum Venaticorum Binaries. ApJ 640(1):466–473, DOI 10.1086/500080, astro-ph/0510652

Bildsten L, Shen KJ, Weinberg NN, Nelemans G (2007) Faint Thermonuclear Supernovae from AM Canum Venaticorum Binaries. ApJL 662(2):L95–L98, DOI 10.1086/519489, astro-ph/0703578

Blanton MR, Moustakas J (2009) Physical Properties and Environments of Nearby Galaxies. ARA&A 47(1):159–210, DOI 10.1146/annurev-astro-082708-101734, 0908.3017

Bond JR, Kofman L, Pogosyan D (1996) How filaments of galaxies are woven into the cosmic web. Nature 380:603–606, DOI 10.1038/380603a0, astro-ph/9512141

Borisova E, Cantalupo S, Lilly SJ, Marino RA, Gallego SG, Bacon R, Blaizot J, Bouché N, Brinchmann J, Carollo CM, Caruana J, Finley H, Herenz EC, Richard J, Schaye J, Straka LA, Turner ML, Urrutia T, Verhamme A, Wisotzki L (2016) ApJ 831:39, DOI 10.3847/0004-637X/831/1/39, 1605.01422

Boselli A, Gavazzi G (2014) On the origin of the faint-end of the red sequence in high-density environments. A&AR 22:74, DOI 10.1007/s00159-014-0074-y, 1411.5513

Boselli A, Boissier S, Cortese L, Gil de Paz A, Seibert M, Madore BF, Buat V, Martin DC (2006) The Fate of Spiral Galaxies in Clusters: The Star Formation History of the Anemic Virgo Cluster Galaxy NGC 4569. ApJ 651(2):811–821, DOI 10.1086/507766, astro-ph/0609020

Branch D, Tammann GA (1992) Type IA supernovae as standard candles. ARA&A 30:359–389

Burrows A (2013) Colloquium: Perspectives on core-collapse supernova theory. Rev Mod Phys 85(1):245–261, DOI 10.1103/RevModPhys.85.245, URL https://link.aps.org/doi/10.1103/RevModPhys.85.245

Cai Z, Fan X, Yang Y, Bian F, Prochaska JX, Zabludoff A, McGreer I, Zheng ZY, Green R, Cantalupo S, Frye B, Hamden E, Jiang L, Kashikawa N, Wang R (2017) Discovery of an Enormous Lyα Nebula in a Massive Galaxy Overdensity at z = 2.3. ApJ 837:71, DOI 10.3847/1538-4357/aa5d14, 1609.04021

Cai Z, Hamden E, Matuszewski M, Prochaska JX, Li Q, Cantalupo S, Arrigoni Battaia F, Martin C, Neill JD, O'Sullivan D, Wang R, Moore A, Morrissey P (2018) Keck/Palomar Cosmic Web Imagers Reveal an Enormous Lyα Nebula in an Extremely Overdense Quasi-stellar Object Pair Field at z = 2.45. ApJL 861:L3, DOI 10.3847/2041-8213/aacce6, 1803.10781

Cantalupo S, Porciani C, Lilly SJ, Miniati F (2005) Fluorescent Lyα Emission from the High-Redshift Intergalactic Medium. ApJ 628:61–75, DOI 10.1086/430758, astro-ph/0504015

Cantalupo S, Arrigoni-Battaia F, Prochaska JX, Hennawi JF, Madau P (2014) A cosmic web filament revealed in Lyman-α emission around a luminous high-redshift quasar. Nature 506:63–66, DOI 10.1038/nature12898, 1401.4469

Christensen L, Jahnke K, Wisotzki L, Sánchez SF (2006) Extended Lyman-α emission around bright quasars. A&A 459:717–729, DOI 10.1051/0004-6361:20065318, arXiv:astro-ph/0603835

Cimatti A, Cassata P, Pozzetti L, Kurk J, Mignoli M, Renzini A, Daddi E, Bolzonella M, Brusa M, Rodighiero G, Dickinson M, Franceschini A, Zamorani G, Berta S, Rosati P, Halliday C (2008) GMASS ultradeep spectroscopy of galaxies at z ∼ 2. II. Superdense passive galaxies: how did they form and evolve? A&A 482:21–42, DOI 10.1051/0004-6361:20078739, 0801.1184

Coogan RT, Daddi E, Sargent MT, Strazzullo V, Valentino F, Gobat R, Magdis G, Bethermin M, Pannella M, Onodera M, Liu D, Cimatti A, Dannerbauer H, Carollo M, Renzini A, Tremou E (2018) Merger-driven star formation activity in Cl J1449+0856 at z = 1.99 as seen by ALMA and JVLA. MNRAS 479:703–729, DOI 10.1093/mnras/sty1446, 1805.09789

Croton DJ, Springel V, White SDM, De Lucia G, Frenk CS, Gao L, Jenkins A, Kauffmann G, Navarro JF, Yoshida N (2006) The many lives of active galactic nuclei: cooling flows, black holes and the luminosities and colours of galaxies. MNRAS 365(1):11–28, DOI 10.1111/j.1365-2966.2005.09675.x, astro-ph/0508046

Daddi E, Dickinson M, Morrison G, Chary R, Cimatti A, Elbaz D, Frayer D, Renzini A, Pope A, Alexander DM, Bauer FE, Giavalisco M, Huynh M, Kurk J, Mignoli M (2007) Multiwavelength Study of Massive Galaxies at z ∼ 2. I. Star Formation and Galaxy Growth. ApJ 670:156–172, DOI 10.1086/521818, 0705.2831

Dannerbauer H, Lehnert MD, Emonts B, Ziegler B, Altieri B, De Breuck C, Hatch N, Kodama T, Koyama Y, Kurk JD, Matiz T, Miley G, Narayanan D, Norris RP, Overzier R, Röttgering HJA, Sargent M, Seymour N, Tanaka M, Valtchanov I, Wylezalek D (2017) The implications of the surprising existence of a large, massive CO disk in a distant protocluster. A&A 608:A48, DOI 10.1051/0004-6361/201730449, 1701.05250

Dekel A, Birnboim Y (2006) Galaxy bimodality due to cold flows and shock heating. MNRAS 368(1):2–20, DOI 10.1111/j.1365-2966.2006.10145.x, astro-ph/0412300

Dennehy C, Alvarez-Salazar OS (2018) Spacecraft Micro-Vibration: A Survey of Problems, Experiences, Potential Solutions, and Some Lessons Learned. Tech. Rep. NASA/TM-2018-220075, NASA

Deshpande A, Lützgendorf N, Ferruit P, Giardino G, Alves de Oliveira C, Birkmann SM, Böker T, Puga E, Rawle TD, Sirianni M, te Plate M (2018) The contrast performance of the NIRSpec micro shutters and its impact on NIRSpec integral field observations. In: Proc. SPIE , Society of Photo-Optical Instrumentation Engineers (SPIE) Conference Series, vol 10698, p 106985N, DOI 10.1117/12.2312425

Dressler A (1980) Galaxy morphology in rich clusters: implications for the formation and evolution of galaxies. ApJ 236:351–365, DOI 10.1086/157753

Farina EP, Venemans BP, Decarli R, Hennawi JF, Walter F, Bañados E, Mazzucchelli C, Cantalupo S, Arrigoni-Battaia F, McGreer ID (2017) Mapping the Lyα Emission around a z ∼ 6.6 QSO with MUSE: Extended Emission and a Companion at a Close Separation. ApJ 848:78, DOI 10.3847/1538-4357/aa8df4, 1709.06096

Farina EP, Arrigoni-Battaia F, Costa T, Walter F, Hennawi JF, Drake AB, Decarli R, Gutcke TA, Mazzucchelli C, Neeleman M, Georgiev I, Eilers AC, Davies FB, Bañados E, Fan X, Onoue M, Schindler JT, Venemans BP, Wang F, Yang J, Rabien S, Busoni L (2019) The REQUIEM Survey. I. A Search for Extended Lyα Nebular Emission Around 31 z$\gtrsim$5.7 Quasars. ApJ 887(2):196, DOI 10.3847/1538-4357/ab5847, 1911.08498

Faucher-Giguère CA (2020) A cosmic UV/X-ray background model update. MNRAS 493(2):1614–1632, DOI 10.1093/mnras/staa302, 1903.08657

Fink M, Röpke FK, Hillebrandt W, Seitenzahl IR, Sim SA, Kromer M (2010) Double-detonation sub-Chandrasekhar supernovae: can minimum helium shell masses detonate the core? A&A 514:A53, DOI 10.1051/0004-6361/200913892, 1002.2173

Fossati M, Fumagalli M, Boselli A, Gavazzi G, Sun M, Wilman DJ (2016) MUSE sneaks a peek at extreme ram-pressure stripping events - II. The physical properties of the gas tail of ESO137-001. MNRAS 455:2028–2041, DOI 10.1093/mnras/stv2400, 1510.04283

France K, Fleming B, West G, McCand liss SR, Bolcar MR, Harris W, Moustakas L, O'Meara JM, Pascucci I, Rigby J, Schiminovich D, Tumlinson J (2017) The LUVOIR Ultraviolet Multi-Object Spectrograph (LUMOS): instrument definition and design. In: Proc. SPIE , Society of Photo-Optical Instrumentation Engineers (SPIE) Conference Series, vol 10397, p 1039713, DOI 10.1117/12.2272025, 1709.06141

Fumagalli M, Krumholz MR, Prochaska JX, Gavazzi G, Boselli A (2009) Molecular Hydrogen Deficiency in H I-poor Galaxies and its Implications for Star Formation. ApJ 697(2):1811–1821, DOI 10.1088/0004-637X/697/2/1811, 0903.3950

Fumagalli M, Fossati M, Hau GKT, Gavazzi G, Bower R, Sun M, Boselli A (2014) MUSE sneaks a peek at extreme ram-pressure stripping events - I. A kinematic study of the archetypal galaxy ESO137-001. MNRAS 445(4):4335–4344, DOI 10.1093/mnras/stu2092, 1407.7527

Gal-Yam A, Arcavi I, Ofek EO, Ben-Ami S, Cenko SB, Kasliwal MM, Cao Y, Yaron O, Tal D, Silverman JM, Horesh A, De Cia A, Taddia F, Sollerman J, Perley D, Vreeswijk PM, Kulkarni SR, Nugent PE, Filippenko AV, Wheeler JC (2014) A Wolf-Rayet-like progenitor of SN 2013cu from spectral observations of a stellar wind. Nature 509(7501):471–474, DOI 10.1038/nature13304, 1406.7640

Gallego SG, Cantalupo S, Lilly S, Marino RA, Pezzulli G, Schaye J, Wisotzki L, Bacon R, Inami H, Akhlaghi M, Tacchella S, Richard J, Bouche NF, Steinmetz M, Carollo M (2018) Stacking the Cosmic Web in fluorescent Ly α emission with MUSE. MNRAS 475:3854–3869, DOI 10.1093/mnras/sty037, 1706.03785

Gänsicke BT, Szkody P, de Martino D, Beuermann K, Long KS, Sion EM, Knigge C, Marsh T, Hubeny I (2003) Anomalous Ultraviolet Line Flux Ratios in the Cataclysmic Variables 1RXS J232953.9+062814, CE 315, BZ Ursae Majoris, and EY Cygni, Observed with the Hubble Space Telescope Space Telescope Imaging Spectrograph. ApJ 594(1):443–448, DOI 10.1086/376902, astro-ph/0305264

Gänsicke BT, Long KS, Barstow MA, Hubeny I (2006) FUSE and HST STIS Far-Ultraviolet Observations of AM Herculis in an Extended Low State. ApJ 639(2):1039–1052, DOI 10.1086/499358, astro-ph/0511100

Garin M, Heinonen J, Werner L, Pasanen TP, Vahanissi V, Haarahiltunen A, Juntunen M, Savin H (2019) Black silicon UV photodiodes achieve $\gtrsim$130% external quantum efficiency. arXiv e-prints arXiv:1907.13397, 1907.13397

Gavazzi G, Jaffe W (1985) Enhanced star formation in cluster galaxies. ApJL 294:L89–L92, DOI 10.1086/184515

Gould A, Weinberg DH (1996) Imaging the Forest of Lyman Limit Systems. ApJ 468:462–+, DOI 10.1086/177707, astro-ph/9512138

Green JC, Froning CS, Osterman S, Ebbets D, Heap SH, Leitherer C, Linsky JL, Savage BD, Sembach K, Shull JM, Siegmund OHW, Snow TP, Spencer J, Stern SA, Stocke J, Welsh B, Béland S, Burgh EB, Danforth C, France K, Keeney B, McPhate J, Penton SV, Andrews J, Brownsberger K, Morse J, Wilkinson E (2012) The Cosmic Origins Spectrograph. ApJ 744(1):60, DOI 10.1088/0004-637X/744/1/60, 1110.0462

Green MJ, Marsh TR, Steeghs DTH, Kupfer T, Ashley RP, Bloemen S, Breedt E, Campbell HC, Chakpor A, Copperwheat CM, Dhillon VS, Hallinan G, Hardy LK, Hermes JJ, Kerry P, Littlefair SP, Milburn J, Parsons SG, Prasert N, van Roestel J, Sahman DI, Singh N (2018) High-speed photometry of Gaia14aae: an eclipsing AM CVn that challenges formation models. MNRAS 476(2):1663–1679, DOI 10.1093/mnras/sty299, 1802.00499

Groh JH (2014) Early-time spectra of supernovae and their precursor winds: The luminous blue variable/yellow hypergiant progenitor of SN 2013cu. A&A 572:L11, DOI 10.1051/0004-6361/201424852, URL http://www.aanda.org/10.1051/0004-6361/201424852

Gunn JE, Gott I J Richard (1972) On the Infall of Matter Into Clusters of Galaxies and Some Effects on Their Evolution. ApJ 176:1, DOI 10.1086/151605

Haardt F, Madau P (2012) Radiative Transfer in a Clumpy Universe. IV. New Synthesis Models of the Cosmic UV/X-Ray Background. ApJ 746:125, DOI 10.1088/0004-637X/746/2/125, 1105.2039

Haiman Z, Rees MJ (2001) Extended Lyα Emission around Young Quasars: A Constraint on Galaxy Formation. ApJ 556:87–92, DOI 10.1086/321567, arXiv:astro-ph/0101174

Hamanowicz A, Péroux C, Zwaan MA, Rahmani H, Pettini M, York DG, Klitsch A, Augustin R, Krogager JK, Kulkarni V, Fresco Ar, Biggs AD, Milliard B, Vernet JDR (2020) MUSE-ALMA haloes V: physical properties and environment of z $\leq$ 1.4 H I quasar absorbers. MNRAS 492(2):2347–2368, DOI 10.1093/mnras/stz3590, 1912.08699

Hamden ET, Jewell AD, Shapiro CA, Cheng SR, Goodsall TM, Hennessy J, Hoenk M, Jones T, Gordon S, Ong HR, Schiminovich D, Martin DC, Nikzad S (2016) Charge-coupled devices detectors with high quantum efficiency at UV wavelengths. Journal of Astronomical Telescopes, Instruments, and Systems 2:036003, DOI 10.1117/1.JATIS.2.3.036003, 1701.02733

Hamden ET, Hoadley K, Martin DC, Schiminovich D, Milliard B, Nikzad S, Augustin R, Balard P, Blanchard P, Bray N, Crabill M, Evrard J, Gomes A, Grange R, Gross J, Jewell A, Kyne G, Limon M, Lingner N, Matuszewski M, Melso N, Mirc F, Montel J, Ong HR, O'Sullivan D, Pascal S, Perot E, Picouet V, Saccoccio M, Smiley B, Soors X, Tapie P, Vibert D, Zenone I, Zorilla J (2019) FIREBall-2: advancing TRL while doing proof-of-concept astrophysics on a suborbital platform. arXiv e-prints arXiv:1905.00433, 1905.00433

Haynes MP (1985) H I deficiency in the Virgo cluster. In: European Southern Observatory Conference and Workshop Proceedings, vol 20, pp 45–50

Heckman TM, Miley GK, Lehnert MD, van Breugel W (1991) Spatially resolved optical images of high-redshift quasi-stellar objects. ApJ 370:78–101, DOI 10.1086/169794

Hennawi JF, Prochaska JX, Cantalupo S, Arrigoni-Battaia F (2015) Quasar quartet embedded in giant nebula reveals rare massive structure in distant universe. Science 348:779–783, DOI 10.1126/science.aaa5397, 1505.03786

Hopkins PF, Kereš D, Murray N, Quataert E, Hernquist L (2012) Stellar feedback and bulge formation in clumpy discs. MNRAS 427:968–978, DOI 10.1111/j.1365-2966.2012.21981.x, 1111.6591

Hu EM, Cowie LL (1987) The distribution of gas and galaxies around the distant quasar PKS 1614 + 051. ApJL 317:L7–L12, DOI 10.1086/184902

Ivanova N, Heinke CO, Rasio FA, Taam RE, Belczynski K, Fregeau J (2006) Formation and evolution of compact binaries in globular clusters - I. Binaries with white dwarfs. MNRAS 372(3):1043–1059, DOI 10.1111/j.1365-2966.2006.10876.x, astro-ph/0604085

Johansson PH, Burkert A, Naab T (2009) The Evolution of Black Hole Scaling Relations in Galaxy Mergers. ApJL 707(2):L184–L189, DOI 10.1088/0004-637X/707/2/L184, 0910.2232

Kendrick SE, Woodruff RA, Hull T, Heap SR, Kutyrev A (2019) Science capabilities enabled by the CETUS NUV multi-object spectrometer and NUV/FUV camera and the driving technologies. In: Proc. SPIE , Society of Photo-Optical Instrumentation Engineers (SPIE) Conference Series, vol 11115, p 1111504, DOI 10.1117/12.2529790

Kennicutt RC Jr (1998) The Global Schmidt Law in Star-forming Galaxies. ApJ 498:541–552, DOI 10.1086/305588, astro-ph/9712213

Khaire V, Srianand R (2019) New synthesis models of consistent extragalactic background light over cosmic time. MNRAS 484(3):4174–4199, DOI 10.1093/mnras/stz174, 1801.09693

Khazov D, Yaron O, Gal-Yam A, Manulis I, Rubin A, Kulkarni SR, Arcavi I, Kasliwal MM, Ofek EO, Cao Y, Perley D, Sollerman J, Horesh A, Sullivan M, Filippenko AV, Nugent PE, Howell DA, Cenko SB, Silverman JM, Ebeling H, Taddia F, Johansson J, Laher RR, Surace J, Rebbapragada UD, Wozniak PR, Matheson T (2016) Flash Spectroscopy: Emission Lines from the Ionized Circumstellar Material around <10-day-old Type II Supernovae. ApJ 818(1):3, DOI 10.3847/0004-637X/818/1/3, URL http://stacks.iop.org/0004-637X/818/i=1/a=3

Knigge C (2012) Cataclysmic variables in globular clusters. 83:549, 1112.1074

Knigge C, Zurek DR, Shara MM, Long KS (2002) A Far-Ultraviolet Survey of 47 Tucanae. I. Imaging. ApJ 579(2):752–759, DOI 10.1086/342835, astro-ph/0207060

Kollmeier JA, Zheng Z, Davé R, Gould A, Katz N, Miralda-Escudé J, Weinberg DH (2010) Lyα Emission from Cosmic Structure. I. Fluorescence. ApJ 708:1048–1075, DOI 10.1088/0004-637X/708/2/1048, 0907.0704

Krogager JK, Møller P, Fynbo JPU, Noterdaeme P (2017) Consensus report on 25 yr of searches for damped Ly α galaxies in emission: confirming their metallicity-luminosity relation at z $\gtrsim$ 2. MNRAS 469(3):2959–2981, DOI 10.1093/mnras/stx1011, 1704.08075

Kupfer T, Korol V, Shah S, Nelemans G, Marsh TR, Ramsay G, Groot PJ, Steeghs DTH, Rossi EM (2018) LISA verification binaries with updated distances from Gaia Data Release 2. MNRAS 480:302–309, 1805.00482

Larson RB, Tinsley BM, Caldwell CN (1980) The evolution of disk galaxies and the origin of S0 galaxies. ApJ 237:692–707, DOI 10.1086/157917

Leclercq F, Bacon R, Verhamme A, Garel T, Blaizot J, Brinchmann J, Cantalupo S, Claeyssens A, Conseil S, Contini T, Hashimoto T, Herenz EC, Kusakabe H, Marino RA, Maseda M, Matthee J, Mitchell P, Pezzulli G, Richard J, Schmidt KB, Wisotzki L (2020) The MUSE Hubble Ultra Deep Field Survey. XIII. Spatially resolved spectral properties of Lyman α haloes around star-forming galaxies at z $\gtrsim$ 3. A&A 635:A82, DOI 10.1051/0004-6361/201937339, 2002.05731

Lemaitre G, Grange R, Quiret S, Milliard B, Pascal S, Lamandé V (2019) Multi Object Spectrograph of the Fireball-II Balloon Experiment. arXiv e-prints arXiv:1903.02218, 1903.02218

Li W, Chornock R, Leaman J, Filippenko AV, Poznanski D, Wang X, Ganeshalingam M, Mannucci F (2011) Nearby supernova rates from the Lick Observatory Supernova Search - III. The rate-size relation, and the rates as a function of galaxy Hubble type and colour. MNRAS 412(3):1473–1507, DOI 10.1111/j.1365-2966.2011.18162.x, 1006.4613

Long KS, Sion EM, Gänsicke BT, Szkody P (2004) WZ Sagittae: Hubble Space Telescope Spectroscopy of the Cooling of the White Dwarf after the 2001 Outburst. ApJ 602(2):948–959, DOI 10.1086/381121, astro-ph/0310864

Lusso E, Fumagalli M, Fossati M, Mackenzie R, Bielby RM, Arrigoni Battaia F, Cantalupo S, Cooke R, Cristiani S, Dayal P, D'Odorico V, Haardt F, Lofthouse E, Morris S, Peroux C, Prichard L, Rafelski M, Simcoe R, Swinbank AM, Theuns T (2019) The MUSE Ultra Deep Field (MUDF) - I. Discovery of a group of Lyα nebulae associated with a bright z $\sim$ 3.23 quasar pair. MNRAS 485:L62–L67, DOI 10.1093/mnrasl/slz032, 1903.00483

LUVOIR team (2018) The LUVOIR Mission Concept Study Interim Report. arXiv e-prints arXiv:1809.09668, 1809.09668

Madau P, Dickinson M (2014) Cosmic Star-Formation History. ARA&A 52:415–486, DOI 10.1146/annurev-astro-081811-125615, 1403.0007

Malavasi N, Arnouts S, Vibert D, de la Torre S, Moutard T, Pichon C, Davidzon I, Kraljic K, Bolzonella M, Guzzo L, Garilli B, Scodeggio M, Granett BR, Abbas U, Adami C, Bottini D, Cappi A, Cucciati O, Franzetti P, Fritz A, Iovino A, Krywult J, Le Brun V, Le Fèvre O, Maccagni D, Małek K, Marulli F, Polletta M, Pollo A, Tasca L, Tojeiro R, Vergani D, Zanichelli A, Bel J, Branchini E, Coupon J, De Lucia G, Dubois Y, Hawken A, Ilbert O, Laigle C, Moscardini L, Sousbie T, Treyer M, Zamorani G (2017) The VIMOS Public Extragalactic Redshift Survey (VIPERS): galaxy segregation inside filaments at z $\sim$ 0.7. MNRAS 465(4):3817–3822, DOI 10.1093/mnras/stw2864, 1611.07045

Maoz D, Mannucci F (2012) Type-Ia Supernova Rates and the Progenitor Problem: A Review. PASA 29(4):447–465, DOI 10.1071/AS11052, 1111.4492

Martig M, Bournaud F, Teyssier R, Dekel A (2009) Morphological Quenching of Star Formation: Making Early-Type Galaxies Red. ApJ 707:250–267, DOI 10.1088/0004-637X/707/1/250, 0905.4669

Martin CD, Matuszewski M, Rahman S, Morrissey P, Moore A, Schiminovich D, Milliard B, Frank S, Deharveng J, Peroux C, CWI Team, FIREBALL Team, KCWI Team, ISTOS Team (2011) The IGM

Project: Searching For IGM Emission Over 0<z<4 With FIREBALL And CWI. In: American Astronomical Society Meeting Abstracts #217, American Astronomical Society Meeting Abstracts, vol 217, p 426.04

Martin DC, Chang D, Matuszewski M, Morrissey P, Rahman S, Moore A, Steidel CC (2014) Intergalactic Medium Emission Observations with the Cosmic Web Imager. I. The Circum-QSO Medium of QSO 1549+19, and Evidence for a Filamentary Gas Inflow. ApJ 786:106, DOI 10.1088/0004-637X/786/2/106, 1402.4816

Maund JR, Fraser M, Ergon M, Pastorello A, Smartt SJ, Sollerman J, Benetti S, Botticella MT, Bufano F, Danziger IJ, Kotak R, Magill L, Stephens AW, Valenti S (2011) The Yellow Supergiant Progenitor of the Type II Supernova 2011dh in M51. ApJ 739(2):L37, DOI 10.1088/2041-8205/739/2/L37, URL http://iopscience.iop.org/2041-8205/739/2/L37

Meeker SR, Mazin BA, Walter AB, Strader P, Fruitwala N, Bockstiegel C, Szypryt P, Ulbricht G, Coiffard G, Bumble B, Cancelo G, Zmuda T, Treptow K, Wilcer N, Collura G, Dodkins R, Lipartito I, Zobrist N, Bottom M, Shelton JC, Mawet D, van Eyken JC, Vasisht G, Serabyn E (2018) DARKNESS: A Microwave Kinetic Inductance Detector Integral Field Spectrograph for High-contrast Astronomy. PASP 130(988):065001, DOI 10.1088/1538-3873/aab5e7, 1803.10420

Meiksin AA (2009) The physics of the intergalactic medium. Reviews of Modern Physics 81:1405–1469, DOI 10.1103/RevModPhys.81.1405, 0711.3358

Møller P, Warren SJ, Fall SM, Jakobsen P, Fynbo JU (2000) SPSF subtraction II: The extended Lyα emission of a radio quiet QSO. The Messenger 99:33–35

Morales-Rueda L, Marsh TR, Steeghs D, Unda-Sanzana E, Wood JH, North RC (2003) New results on GP Com. A&A 405:249–261, DOI 10.1051/0004-6361:20030552, astro-ph/0304265

Morrissey P, Matuszewski M, Martin C, Moore A, Adkins S, Epps H, Bartos R, Cabak J, Cowley D, Davis J, Delacroix A, Fucik J, Hilliard D, James E, Kaye S, Lingner N, Neill JD, Pistor C, Phillips D, Rockosi C, Weber B (2012) The Keck Cosmic Web Imager: a capable new integral field spectrograph for the W. M. Keck Observatory 8446:844613, DOI 10.1117/12.924729

Nakar E, Sari R (2010) Early Supernovae Light Curves Following the Shock Breakout. ApJ 725(1):904, DOI 10.1088/0004-637X/725/1/904, URL http://iopscience.iop.org/0004-637X/725/1/904

Nelemans G, Yungelson LR, van der Sluys MV, Tout CA (2010) The chemical composition of donors in AM CVn stars and ultracompact X-ray binaries: observational tests of their formation. MNRAS 401(2):1347–1359, DOI 10.1111/j.1365-2966.2009.15731.x, 0909.3376

Noterdaeme P, Petitjean P, Carithers WC, Pâris I, Font-Ribera A, Bailey S, Aubourg E, Bizyaev D, Ebelke G, Finley H, Ge J, Malanushenko E, Malanushenko V, Miralda-Escudé J, Myers AD, Oravetz D, Pan K, Pieri MM, Ross NP, Schneider DP, Simmons A, York DG (2012) Column density distribution and cosmological mass density of neutral gas: Sloan Digital Sky Survey-III Data Release 9. A&A 547:L1, DOI 10.1051/0004-6361/201220259, 1210.1213

Pala AF, Gänsicke BT, Townsley D, Boyd D, Cook MJ, De Martino D, Godon P, Haislip JB, Henden AA, Hubeny I, Ivarsen KM, Kafka S, Knigge C, LaCluyze AP, Long KS, Marsh TR, Monard B, Moore JP, Myers G, Nelson P, Nogami D, Oksanen A, Pickard R, Poyner G, Reichart DE, Rodriguez Perez D, Schreiber MR, Shears J, Sion EM, Stubbings R, Szkody P, Zorotovic M (2017) Effective temperatures of cataclysmic-variable white dwarfs as a probe of their evolution. MNRAS 466(3):2855–2878, DOI 10.1093/mnras/stw3293, 1701.02738

Pala AF, Gänsicke BT, Breedt E, Knigge C, Hermes JJ, Gentile Fusillo NP, Hollands MA, Naylor T, Pelisoli I, Schreiber MR, Toonen S, Aungwerojwit A, Cukanovaite E, Dennihy E, Manser CJ, Pretorius ML, Scaringi S, Toloza O (2020) A Volume-limited Sample of Cataclysmic Variables from Gaia DR2: Space Density and Population Properties. MNRAS 494(3):3799–3827, DOI 10.1093/mnras/staa764, 1907.13152

Peng Y, Maiolino R, Cochrane R (2015) Strangulation as the primary mechanism for shutting down star formation in galaxies. Nature 521(7551):192–195, DOI 10.1038/nature14439, 1505.03143

Peng Yj, Lilly SJ, Kovač K, Bolzonella M, Pozzetti L, Renzini A, Zamorani G, Ilbert O, Knobel C, Iovino A, Maier C, Cucciati O, Tasca L, Carollo CM, Silverman J, Kampczyk P, de Ravel L, Sanders D, Scoville N, Contini T, Mainieri V, Scodeggio M, Kneib JP, Le Fèvre O, Bardelli S, Bongiorno A, Caputi K, Coppa G, de la Torre S, Franzetti P, Garilli B, Lamareille F, Le Borgne JF, Le Brun V, Mignoli M, Perez Montero E, Pello R, Ricciardelli E, Tanaka M, Tresse L, Vergani D, Welikala N, Zucca E, Oesch P, Abbas U, Barnes L, Bordoloi R, Bottini D, Cappi A, Cassata P, Cimatti A, Fumana M, Hasinger G, Koekemoer A, Leauthaud A, Maccagni D, Marinoni C, McCracken H, Memeo P, Meneux B, Nair P, Porciani C, Presotto V, Scaramella R (2010) Mass and Environment as Drivers of Galaxy Evolution in SDSS and zCOSMOS and the Origin of the Schechter Function. ApJ 721:193–221, DOI 10.1088/0004-637X/721/1/193, 1003.4747

Perlmutter S, Aldering G, Goldhaber G, Knop RA, Nugent P, Castro PG, Deustua S, Fabbro S, Goobar A, Groom DE, Hook IM, Kim AG, Kim MY, Lee JC, Nunes NJ, Pain R, Pennypacker CR, Quimby R, Lidman C, Ellis RS, Irwin M, McMahon RG, Ruiz-Lapuente P, Walton N, Schaefer B, Boyle BJ, Filippenko AV, Matheson T, Fruchter AS, Panagia N, Newberg HJM, Couch WJ, Project TSC (1999) Measurements of Ω and Λ from 42 High-Redshift Supernovae. ApJ 517(2):565–586, DOI 10.1086/307221, astro-ph/9812133

Péroux C, Howk JC (2020) The Cosmic Baryon and Metal Cycles. ARA&A 58:363–406, DOI 10.1146/annurev-astro-021820-120014, 2011.01935

Pieri MM, Mortonson MJ, Frank S, Crighton N, Weinberg DH, Lee KG, Noterdaeme P, Bailey S, Busca N, Ge J, Kirkby D, Lundgren B, Mathur S, Pâris I, Palanque-Delabrouille N, Petitjean P, Rich J, Ross NP, Schneider DP, York DG (2014) Probing the circumgalactic medium at high-redshift using composite BOSS spectra of strong Lyman α forest absorbers. MNRAS 441(2):1718–1740, DOI 10.1093/mnras/stu577, 1309.6768

Quijada MA, del Hoyo J, Boris DR, Walton SG (2017) Improved mirror coatings for use in the Lyman Ultraviolet to enhance astronomical instrument capabilities. In: Society of Photo-Optical Instrumentation Engineers (SPIE) Conference Series, Society of Photo-Optical Instrumentation Engineers (SPIE) Conference Series, vol 10398, p 103980Z, DOI 10.1117/12.2274790

Quiret S, Péroux C, Zafar T, Kulkarni VP, Jenkins EB, Milliard B, Rahmani H, Popping A, Rao SM, Turnshek DA, Monier EM (2016) The ESO UVES advanced data products quasar sample - VI. Sub-damped Lyman α metallicity measurements and the circumgalactic medium. MNRAS 458(4):4074–4121, DOI 10.1093/mnras/stw524, 1602.02564

Rabinak I, Waxman E (2011) The Early UV/Optical Emission from Core-collapse Supernovae. ApJ 728(1):63, DOI 10.1088/0004-637X/728/1/63, URL http://iopscience.iop.org/0004-637X/728/1/63

Rahmani H, Péroux C, Turnshek DA, Rao SM, Quiret S, Hamilton TS, Kulkarni VP, Monier EM, Zafar T (2016) MNRAS 463(1):980–1007, DOI 10.1093/mnras/stw1965, 1609.03843

Rauscher BJ, Canavan ER, Moseley SH, Sadleir JE, Stevenson T (2016) Detectors and cooling technology for direct spectroscopic biosignature characterization. Journal of Astronomical Telescopes, Instruments, and Systems 2:041212, DOI 10.1117/1.JATIS.2.4.041212, 1607.05708

Rees MJ (1988) Quasars as probes of gas in extended protogalaxies. MNRAS 231:91p–95p, DOI 10.1093/mnras/231.1.91P

Richard J, Bacon R, Blaizot J, Boissier S, Boselli A, NicolasBouché, Brinchmann J, Castro N, Ciesla L, Crowther P, Daddi E, Dreizler S, Duc PA, Elbaz D, Epinat B, Evans C, Fossati M, Fumagalli M, Garcia M, Garel T, Hayes M, Herrero A, Humphrey A, Jablonka P, Kamann S, Kaper L, Kelz A, Kneib JP, de Koter A, Krajnović D, Kudritzki RP, Langer N, Lardo C, Leclercq F, Lennon D, Mahler G, Martins F, Massey R, Mitchell P, Monreal-Ibero A, Najarro P, Opitom C, Papaderos P, Péroux C, Revaz Y, Roth MM, Rousselot P, Sand er A, Simmonds Wagemann C, Smail I, Swinbank AM, Tramper F, Urrutia T, Verhamme A, Vink J, Walsh J, Weilbacher P, Wendt M, Wisotzki L, Yang B (2019) BlueMUSE: Project Overview and Science Cases. arXiv e-prints arXiv:1906.01657, 1906.01657

Riess AG, Filippenko AV, Challis P, Clocchiatti A, Diercks A, Garnavich PM, Gilliland RL, Hogan CJ, Jha S, Kirshner RP, Leibundgut B, Phillips MM, Reiss D, Schmidt BP, Schommer RA, Smith RC, Spyromilio J, Stubbs C, Suntzeff NB, Tonry J (1998) Observational Evidence from Supernovae for an Accelerating Universe and a Cosmological Constant. AJ 116(3):1009–1038, DOI 10.1086/300499, astro-ph/9805201

Rubin A, Gal-Yam A (2017) Exploring the Efficacy and Limitations of Shock-cooling Models: New Analysis of Type II Supernovae Observed by the Kepler Mission. ApJ 848(1):8, DOI 10.3847/1538-4357/aa8465, URL http://stacks.iop.org/0004-637X/848/i=1/a=8

Sanders DB, Mirabel IF (1996) Luminous Infrared Galaxies. ARA&A 34:749, DOI 10.1146/annurev.astro.34.1.749

Sapir N, Waxman E (2017) UV/Optical Emission from the Expanding Envelopes of Type II Supernovae. ApJ 838(2):130, DOI 10.3847/1538-4357/aa64df, URL http://stacks.iop.org/0004-637X/838/i=2/a=130

Scarlata C, Colbert J, Teplitz HI, Panagia N, Hayes M, Siana B, Rau A, Francis P, Caon A, Pizzella A, Bridge C (2009) The Effect of Dust Geometry on the Lyα Output of Galaxies. ApJL 704(2):L98–L102, DOI 10.1088/0004-637X/704/2/L98, 0909.3847

Schmidt M (1959) The Rate of Star Formation. ApJ 129:243, DOI 10.1086/146614

Schreiber MR, Zorotovic M, Wijnen TPG (2016) Three in one go: consequential angular momentum loss can solve major problems of CV evolution. MNRAS 455(1):L16–L20, DOI 10.1093/mnrasl/slv144, 1510.04294

Shull JM, Danforth CW, Tilton EM (2014) Tracing the Cosmic Metal Evolution in the Low-redshift Intergalactic Medium. ApJ 796(1):49, DOI 10.1088/0004-637X/796/1/49, 1409.6720

Sion EM (1995) The Evolutionary Thermal Response of a White Dwarf to Compressional Heating by Periodic Dwarf Nova Accretion Events. ApJ 438:876, DOI 10.1086/175129

Sion EM, Long KS, Szkody P, Huang M (1994) ApJL 430:L53, DOI 10.1086/187436

Sion EM, Solheim JE, Szkody P, Gaensicke BT, Howell SB (2006) The First Direct Spectroscopic Detection of a White Dwarf Primary in an AM CVn System. ApJL 636(2):L125–L128, DOI 10.1086/500085, astro-ph/0602119

Sion EM, Gänsicke BT, Long KS, Szkody P, Knigge C, Hubeny I, deMartino D, Godon P (2008) Hubble Space Telescope STIS Spectroscopy of Long-Period Dwarf Novae in Quiescence. ApJ 681(1):543–553, DOI 10.1086/586699, 0801.4703

Smartt SJ (2015) Observational Constraints on the Progenitors of Core-Collapse Supernovae: The Case for Missing High-Mass Stars. PASA 32:e016, DOI 10.1017/pasa.2015.17, URL http://adsabs.harvard.edu/abs/2015PASA...32...16S

Smartt SJ, Maund JR, Hendry MA, Tout CA, Gilmore GF, Mattila S, Benn CR (2004) Detection of a Red Supergiant Progenitor Star of a Type II-Plateau Supernova. Sci 303(5657):499–503, DOI 10.1126/science.1092967, URL http://science.sciencemag.org/content/303/5657/499

Smartt SJ, Eldridge JJ, Crockett RM, Maund JR (2009) The death of massive stars - I. Observational constraints on the progenitors of Type II-P supernovae. MNRAS 395:1409–1437, DOI 10.1111/j.1365-2966.2009.14506.x, URL http://adsabs.harvard.edu/abs/2009MNRAS.395.1409S

Speagle JS, Steinhardt CL, Capak PL, Silverman JD (2014) A Highly Consistent Framework for the Evolution of the Star-Forming "Main Sequence" from z ~ 0-6. ApJS 214(2):15, DOI 10.1088/0067-0049/214/2/15, 1405.2041

Stefanov KD, Prest M, Downing M, George E, Bezawada N, Holland AD (2020) Simulations and Design of a Single-Photon CMOS Imaging Pixel Using Multiple Non-Destructive Signal Sampling. arXiv e-prints arXiv:2004.02675, 2004.02675

Steidel CC, Erb DK, Shapley AE, Pettini M, Reddy N, Bogosavljević M, Rudie GC, Rakic O (2010) The Structure and Kinematics of the Circumgalactic Medium from Far-ultraviolet Spectra of z ~ 2-3 Galaxies. ApJ 717:289–322, DOI 10.1088/0004-637X/717/1/289, 1003.0679

Szkody P, Anderson S, Agüeros M, Covarrubias R (2002) Finding CVs in the Sloan Digital Sky Survey: First results. In: Gänsicke BT, Beuermann K, Reinsch K (eds) The Physics of Cataclysmic Variables and Related Objects, Astronomical Society of the Pacific Conference Series, vol 261, p 297

Toft S, Smolčić V, Magnelli B, Karim A, Zirm A, Michalowski M, Capak P, Sheth K, Schawinski K, Krogager JK, Wuyts S, Sanders D, Man AWS, Lutz D, Staguhn J, Berta S, Mccracken H, Krpan J, Riechers D (2014) Submillimeter Galaxies as Progenitors of Compact Quiescent Galaxies. ApJ 782(2):68, DOI 10.1088/0004-637X/782/2/68, 1401.1510

Toloba E, Boselli A, Cenarro AJ, Peletier RF, Gorgas J, Gil de Paz A, Muñoz-Mateos JC (2011) Formation and evolution of dwarf early-type galaxies in the Virgo cluster. I. Internal kinematics. A&A 526:A114, DOI 10.1051/0004-6361/201015344, 1011.2198

Townsley DM, Bildsten L (2003) Measuring White Dwarf Accretion Rates via Their Effective Temperatures. ApJL 596(2):L227–L230, DOI 10.1086/379535, astro-ph/0309208

Townsley DM, Bildsten L (2004) Theoretical Modeling of the Thermal State of Accreting White Dwarfs Undergoing Classical Nova Cycles. ApJ 600(1):390–403, DOI 10.1086/379647, astro-ph/0306080

Townsley DM, Gänsicke BT (2009) Cataclysmic Variable Primary Effective Temperatures: Constraints on Binary Angular Momentum Loss. ApJ 693(1):1007–1021, DOI 10.1088/0004-637X/693/1/1007, 0811.2447

Trujillo I, Fliri J (2016) Beyond 31 mag arcsec^{-2}: The Frontier of Low Surface Brightness Imaging with the Largest Optical Telescopes. ApJ 823(2):123, DOI 10.3847/0004-637X/823/2/123, 1510.04696

Tumlinson J, Peeples MS, Werk JK (2017) The Circumgalactic Medium. ARA&A 55:389–432, DOI 10.1146/annurev-astro-091916-055240, 1709.09180

Valls-Gabaud D, MESSIER Collaboration (2017) The MESSIER surveyor: unveiling the ultra-low surface brightness universe. In: Gil de Paz A, Knapen JH, Lee JC (eds) Formation and Evolution of Galaxy Outskirts, IAU Symposium, vol 321, pp 199–201, DOI 10.1017/S1743921316011388

Van Dyk SD (2017) Supernova Progenitors Observed with HST. In: Alsabti AW, Murdin P (eds) Handbook of Supernovae, Springer International Publishing, Cham, pp 693–719, DOI 10.1007/978-3-319-21846-5_126, URL https://doi.org/10.1007/978-3-319-21846-5_126

Waxman E, Mészáros P, Campana S (2007) GRB 060218: A Relativistic Supernova Shock Breakout. ApJ 667(1):351–357, DOI 10.1086/520715, astro-ph/0702450

Weidinger M, Møller P, Fynbo JPU (2004) The Lyman-α glow of gas falling into the dark matter halo of a z = 3 galaxy. Nature 430:999–1001, DOI 10.1038/nature02793, astro-ph/0408478

Weidinger M, Møller P, Fynbo JPU, Thomsen B (2005) The extended Lyman-α emission surrounding the z = 3.04 radio-quiet QSO1205-30: Primordial infalling gas illuminated by the quasar? A&A 436:825–835, DOI 10.1051/0004-6361:20042304, astro-ph/0503241

White SDM, Frenk CS, Davis M, Efstathiou G (1987) Clusters, filaments, and voids in a universe dominated by cold dark matter. ApJ 313:505–516, DOI 10.1086/164990

Wisotzki L, Bacon R, Brinchmann J, Cantalupo S, Richter P, Schaye J, Schmidt KB, Urrutia T, Weilbacher PM, Akhlaghi M, Bouché N, Contini T, Guiderdoni B, Herenz EC, Inami H, Kerutt J, Leclercq F, Marino RA, Maseda M, Monreal-Ibero A, Nanayakkara T, Richard J, Saust R, Steinmetz M, Wendt M (2018) Nearly all the sky is covered by Lyman-α emission around high-redshift galaxies. Nature 562:229–232, DOI 10.1038/s41586-018-0564-6, 1810.00843

Witstok J, Puchwein E, Kulkarni G, Smit R, Haehnelt MG (2019) Prospects for Observing the Cosmic Web in Lyman-{\alpha} Emission. arXiv e-prints 1905.06954

Woodgate BE, Kimble RA, Bowers CW, Kraemer S, Kaiser ME, Danks AC, Grady JF, Loiacono JJ, Brumfield M, Feinberg L, Gull TR, Heap SR, Maran SP, Lindler D, Hood D, Meyer W, Vanhouten C, Argabright V, Franka S, Bybee R, Dorn D, Bottema M, Woodruff R, Michika D, Sullivan J, Hetlinger J, Ludtke C, Stocker R, Delamere A, Rose D, Becker I, Garner H, Timothy JG, Blouke M, Joseph CL, Hartig G, Green RF, Jenkins EB, Linsky JL, Hutchings JB, Moos HW, Boggess A, Roesler F, Weistrop D (1998) The Space Telescope Imaging Spectrograph Design. PASP 110(752):1183–1204,

DOI 10.1086/316243

Yaron O, Perley DA, Gal-Yam A, Groh JH, Horesh A, Ofek EO, Kulkarni SR, Sollerman J, Fransson C, Rubin A, Szabo P, Sapir N, Taddia F, Cenko SB, Valenti S, Arcavi I, Howell DA, Kasliwal MM, Vreeswijk PM, Khazov D, Fox OD, Cao Y, Gnat O, Kelly PL, Nugent PE, Filippenko AV, Laher RR, Wozniak PR, Lee WH, Rebbapragada UD, Maguire K, Sullivan M, Soumagnac MT (2017) Confined dense circumstellar material surrounding a regular type II supernova. NatPh 13(5):510–517, DOI 10.1038/nphys4025, URL https://www.nature.com/nphys/journal/v13/n5/full/nphys4025.html

Yungelson LR (2008) Evolution of low-mass helium stars in semidetached binaries. Astronomy Letters 34(9):620–634, DOI 10.1134/S1063773708090053, 0804.2780